Energy & Buildings 338 (2025) 115732

Contents lists available at ScienceDirect

Energy & Buildings

journal homepage: www.elsevier.com/locate/enb

Enhancing energy storage capability for renewable energy systems through advanced cement-based supercapacitors☆

Caiyu Zhao [a], Wenkui Dong [a], T.M. Indra Mahlia [b], Long Shi [c], Kejin Wang [d], Surendra P. Shah [e], Wengui Li [a,*]

[a] Centre for Infrastructure Engineering and Safety, School of Civil and Environmental Engineering, The University of New South Wales, NSW 2052, Australia
[b] School of Civil and Environmental Engineering, University of Technology Sydney, NSW 2007, Australia
[c] State Key Laboratory of Fire Science, University of Science and Technology of China, Hefei 230026, China
[d] Department of Civil, Construction and Environment Engineering, Iowa State University, IA 50011, USA
[e] Center for Advanced Construction Materials, Department of Civil Engineering, The University of Texas at Arlington, TX 76019, USA

ARTICLE INFO

Keywords:
Cement-based supercapacitor
Energy storage
Electrochemical performance
Renewable energy
Decarbonization

ABSTRACT

As global warming worsens, countries around the world have developed policies to reduce carbon emissions and accelerate the transition to renewable energy. Recently, cement-based supercapacitors have attracted significant attention due to their low energy consumption and multifunctionality, offering a promising solution for large-scale energy storage in renewable energy systems. This review provides an overview of the advancements, mechanism and characterization of cement-based supercapacitors, followed by an analysis of performance studies on mechanical and electrochemical properties based on cement types, water to cement (W/C) ratio, curing age, additives, and various electrodes of contemporary interest. The progress in overcoming issues related to the energy storage capacity and mechanical properties of polymer modified cement-based electrolytes is analyzed. In addition, high-performance and long-lifespan electrodes modified by nanomaterials and metal oxides are essential for establishing highly efficient cement-based supercapacitors. The multifunctionality of these materials is further discussed, emphasizing mitigating intrinsic contradictions is key to large-scale production and commercialization. Finally, perspectives are provided on the future development requirements of advanced cement-based supercapacitors, focusing on sustainability, economic promotion, social impact, and industrial stability. This review not only provides direction for researchers in renewable energy storage but also offers valuable insights for achieving energy savings and carbon neutrality.

Abbreviations: CA, Aluminate cement; CBSC, Cement-based supercapacitors; CF, Carbon fibers; CNTs, Carbon nanotubes; CoOOH, Cobalt hydroxide; C-S-H, Calcium silicate hydrate; $CuCo_2O_4$, Copper cobalt oxide; CuO, Copper oxide; CV, Cyclic voltammetry; EDL, Electrical double-layer; EDLCs, Electric double layer capacitors; EIS, Electrochemical impedance spectroscopy; Fe_2O_3, Iron oxide; GCD, Galvanostatic charge/discharge; H_2O, Hydrogen oxide; KDP, Potassium carbonate; KOH, Potassium hydroxide; LED, Light emitting diode; LiOTf, Lithium trifluoromethanesulfonate; LLZO, $Li_7La_3Zr_2O_{12}$; MgO, Magnesium oxide; MnO(OH), Manganese hydroxide; MnO_2, Manganese oxide; MPC, Magnesium phosphate cement; NASICON, $Na_{1-x}Zr_2Si_xP_{3-x}O_{12}$; NCM-S, Nickel-cobalt-manganese; Ni, Nickel; $Ni(OH)_2$, Nickel hydroxide; Ni_1Co_1S, Nickel cobalt sulfide; $NiCo_2O_4$, Nickel cobalt oxide; OHP, Outer Helmholtz Plane; OPC, Ordinary Portland cement; PAA, Polyacrylic acid; PAAK, Potassium polyacrylate; PAM, Polyacrylamide; PEG, Polyethylene glycol; PEDOT, Poly(3,4-ethylenedioxythiophene); PEO, Polyethylene oxide; PPy-NTs, polypyrrole nanotubes; PV, Photovoltaics; PVA, Polyvinyl alcohol; rGO, Reduced graphene oxide; SEM, Scanning electron microscope; SnO_2, Tin oxide; SRM, Synchronous reaction method; SSEs, Solid-state electrolytes; W/C ratio, Water-to-cement ratio.

☆ This article is part of a special issue entitled: ‘Decarbonising Built Env’ published in Energy & Buildings.

* Corresponding author: Centre for Infrastructure Engineering and Safety, School of Civil and Environmental Engineering, The University of New South Wales, NSW 2052, Australia.

E-mail address: wengui.li@unsw.edu.au (W. Li).

https://doi.org/10.1016/j.enbuild.2025.115732
Received 27 November 2024; Received in revised form 21 February 2025; Accepted 7 April 2025

1. Introduction

1.1. Importance of cement-based supercapacitors

The global energy system is in the midst of a significant shift from fossil-based to renewable energy sources [1,2]. The environmental pollution caused by fossil fuel energy poses a significant challenge to the global environmental equilibrium and the survival of humanity. At present, countries worldwide are implementing a range of initiatives to transition the economies from fossil fuel dependency to renewable energy systems [3]. Meanwhile, researchers have conducted extensive and in-depth studies on energy transition. Among the most prevalent forms of energy storage is chemical energy storage, including technologies such as lithium-ion batteries, sodium-ion batteries, and similar systems. These technologies demonstrate strong performance in terms of energy storage efficiency and density. However, the limited availability of mineral resources required for battery production poses a significant challenge to scaling up energy storage solutions for widespread use [3–6]. Additionally, renewable energy sources like solar, wind, and ocean energy are often intermittent, leading to fluctuations in power supply. Energy storage systems are essential to address these fluctuations and ensure a stable energy supply.

Cement-based supercapacitors (CBSC) represent a groundbreaking solution in energy storage technology. Their high efficiency, scalability, and environmental sustainability position them as a promising option for addressing energy storage challenges. By integrating energy storage capabilities directly into building materials, CBSC can embed energy storage systems within buildings and infrastructure, offering significant potential for future smart buildings and enhancing grid stability. Furthermore, the abundance and low cost of cement make CBSC highly suitable for large-scale deployment, supporting broader adoption of renewable energy. The development of CBSC holds substantial practical importance in overcoming energy storage hurdles during the global energy transition and advancing sustainable energy goals. This innovative technology not only alleviates the resource limitations of current energy storage systems but also provides a more eco-friendly and cost-effective solution, driving the global energy system toward a comprehensive shift to renewable energy.

Fig. 1 shows the schematic diagram and illustration of the CBSC integrated with PV modules, and electrical loads. The electricity energy generated by photovoltaics (PV) modules through the photovoltaics effect can be stored in cement-based supercapacitors, which can reduce the loss of renewable energy. Power is transmitted to users through a power network connected to energy storage devices, which can further improve the utilization rate of solar energy and thus promote the further development of renewable energy systems.

1.2. CBSC development

Fig. 2 shows a chronology of the development of CBSC since the 2000 s. The period between 2000 and 2010 was the initial research and material exploration stage. The studies on CBSC date back to the work of Luo and Chung on the use of solid composites as electrolytes for structural capacitors in 2001 [7]. They used carbon fiber and epoxy composite as solid electrolytes to fabricate the structural supercapacitor with a specific capacitance of 1.2 $\mu F/m^2$. In 2006, Wetzel et al. [8] investigated three candidate multifunctional materials including structural fuel cells, structural batteries and structural capacitors. The relationship between energy density and stiffness of structural capacitors was measured and the design goal for multifunctionality was represented. The period between 2010 and 2015 was the stage of material modification and technology improvement. Meng and Chung [9] showed the feasibility of the set cement-based battery for the first time. The open circuit voltage, current density and power could reach 0.72 V, 3.8$\mu A/cm^2$ and 1.4 $\mu W/cm^2$, respectively. Then in 2015, Zhang et al. [10] proposed a practical cement-based structural supercapacitor assembled

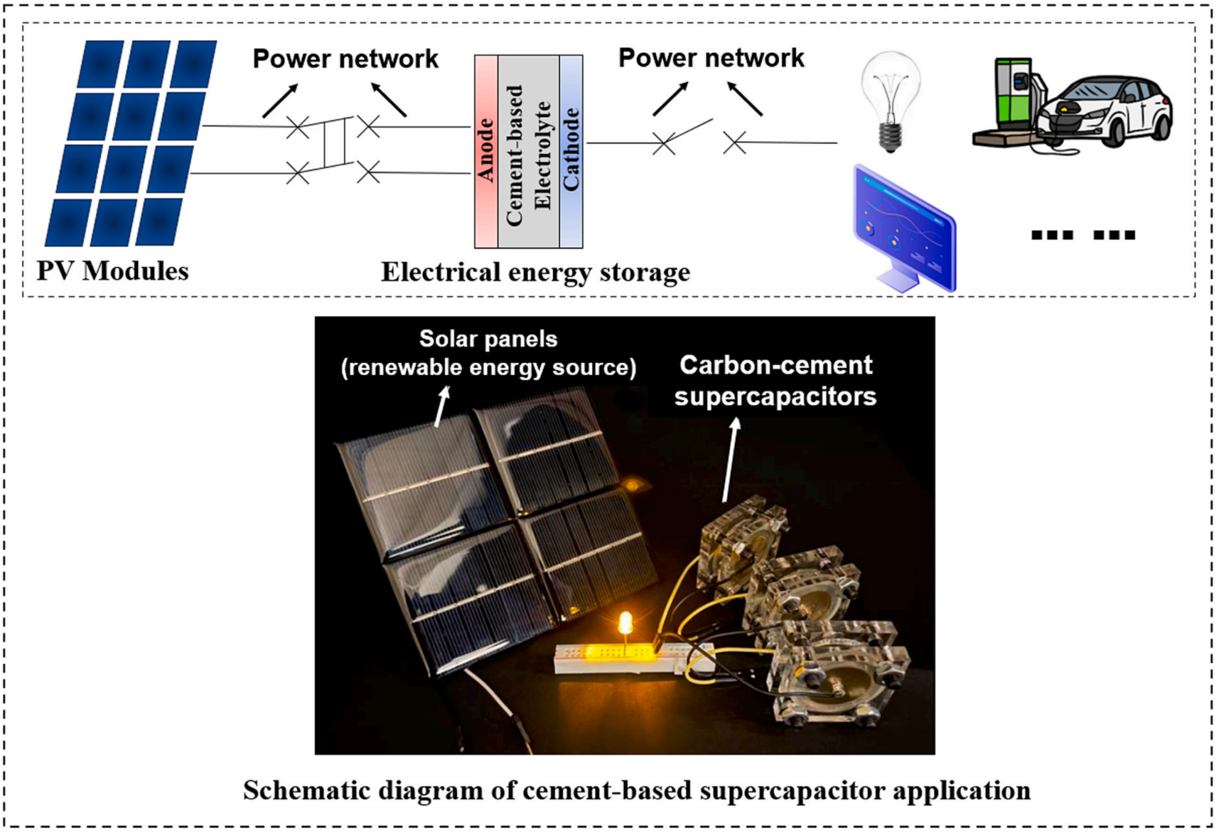

Fig. 1. Schematic illustration of the CBSC integrated with PV modules and electrical loads.

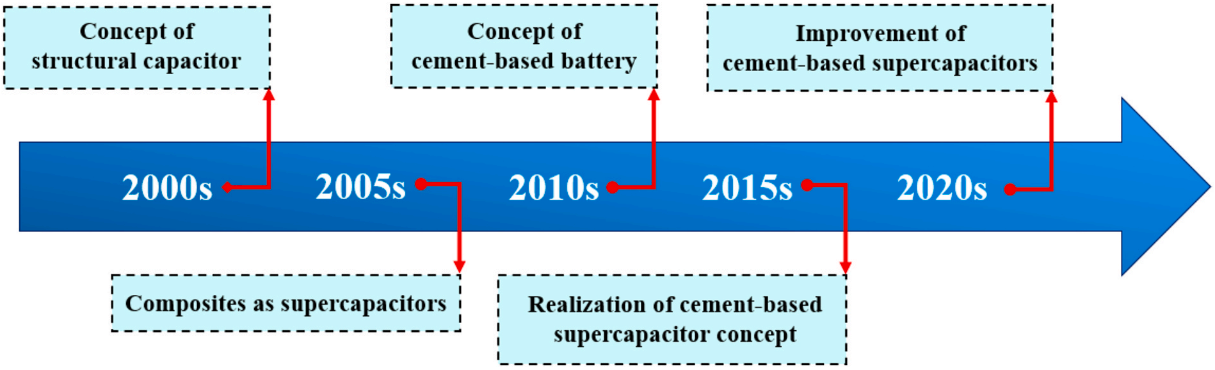

Fig. 2. Chronology of the development of cement-based supercapacitors.

from cement paste and graphene. The maximum specific capacitance was 10F/g with 9.85 MPa of compressive strength. In addition, there was no pseudocapacitance effect so that the CV cures were like an ideal rectangle. The improvement of CBSC was very rapid during the period between 2015 and 2020. The performance of CBSC was enhanced significantly and new composite materials, such as polymer-cement composites, began to attract attention, which exhibited high specific capacitance and stable cycling performance. Subsequently, the optimization of cement-based material design gradually emerged and has been rapidly developed over the past five years.

1.3. *Current state and key issues*

Over the past decade, solid-state electrolytes (SSEs) have emerged as materials of significant scientific and commercial interest for electrical energy storage [11]. The outstanding advantages of SSEs are high charge–discharge rates, high power density and long cycle life, making their application in supercapacitors a popular research topic. As an energy storage solution, supercapacitors can rapidly store and release large amounts of electrical energy, making them highly versatile for applications in electric vehicles, renewable energy systems, and electronic devices. Cement, one of the most widely used materials globally, holds significant potential for the development of supercapacitors. Cement-based supercapacitors (CBSC) not only leverage the multifunctionality of cement but also open new possibilities in advanced energy storage materials [12]. Unlike conventional supercapacitors, the cement matrix in CBSC serves a dual role as both the electrolyte and the separator. During cement hydration, the incorporation of specific additives generates internal pores and networks that enhance ion transport. Additionally, the inherent insulating properties of cement allow it to function effectively as a separator, preventing short circuits between the cathode and anode. Compared to traditional capacitors or supercapacitors, CBSC offer several advantages, including simpler fabrication processes, lower costs, greater durability, and high energy storage capacity, particularly when integrated into large-scale concrete structures and infrastructure.

The key issue of CBSC involve the selection of energy storage components and their cooperation [13]. Shaping the microstructure of the cement matrix is critical for cement-based electrolytes, as it directly influences ion transport pathways and overall electrochemical performance. Further research is also necessary to better understand the compatibility between the cement matrix and various additives [14]. Physical compatibility concerns arise from potential reactions between additives and cement, which could compromise chemical stability. Poor dispersion of additives—due to differences in size, shape, or surface characteristics—can lead to issues such as migration or leaching over time, impacting long-term stability.

Electrode selection is equally vital, as the charge storage capacity and overall performance of a supercapacitor depend heavily on the electrode material [15]. Consequently, much of the current research on CBSCs focuses on optimizing electrode structures and materials. However, the physical contact between high-performance electrodes and the cement matrix is also crucial, as it significantly influences electrochemical properties. This highlights the need for precise control over the preparation process to ensure material consistency. Additionally, some electrode materials can release harmful substances during production, use, or recycling, posing environmental and health risks. Thus, developing eco-friendly materials and sustainable production methods is a key priority for future advancements. For advanced energy storage applications to become commercially viable, large-scale production of materials and processes is essential. While many materials perform well in laboratory settings, scaling them up for industrial manufacturing often presents technical challenges that must be addressed to enable widespread adoption.

1.4. *Methodology and scope*

This review aims to analyze the recent advancements in cement-based supercapacitors and seeks to provide insights into future research directions. A comprehensive literature search was conducted using databases including Google Scholar, Web of Science and Scopus. The search focused on articles using keywords such as “cement-based supercapacitors”, “solid state electrolytes”, “conductivity of cement” and “electrodes of solid-state supercapacitor”.

The articles were included if they (1) analyzed and discussed the application of additives in cement-based materials for energy storage, (2) provided characterization results on physical and chemical properties, (3) provided experimental data on mechanical and electrochemical properties, (4) provided working mechanism of all-solid-state electrolytes, and (5) were published in peer-reviewed journals. Preference was given to studies that conducted comprehensive electrochemical testing, including CV, GCD, EIS and long-term stability tests, and compressive strength tests. For each selected study, data related to compressive strength, ionic conductivity, specific capacitance and microstructures were extracted and analyzed. The analysis was performed to discuss the impact of polymer additives and other factors on the different performance of CBSC.

Currently, there is a notable lack of review articles that comprehensively analyze the development, challenges, and prospects of CBSC. To address this gap, this study begins by examining the fundamental principles of CBSCs, followed by an exploration of their unique characteristics. Statistical analysis is then conducted on data related to their mechanical and electrochemical properties. Additionally, multifunctionality and potential applications of CBSC in renewable energy storage are analyzed. Finally, the challenges and future perspectives of CBSC technology are discussed, offering a comprehensive perspective on its current advancements and potential for future development. The framework of cement-based supercapacitors is shown in Fig. 3.

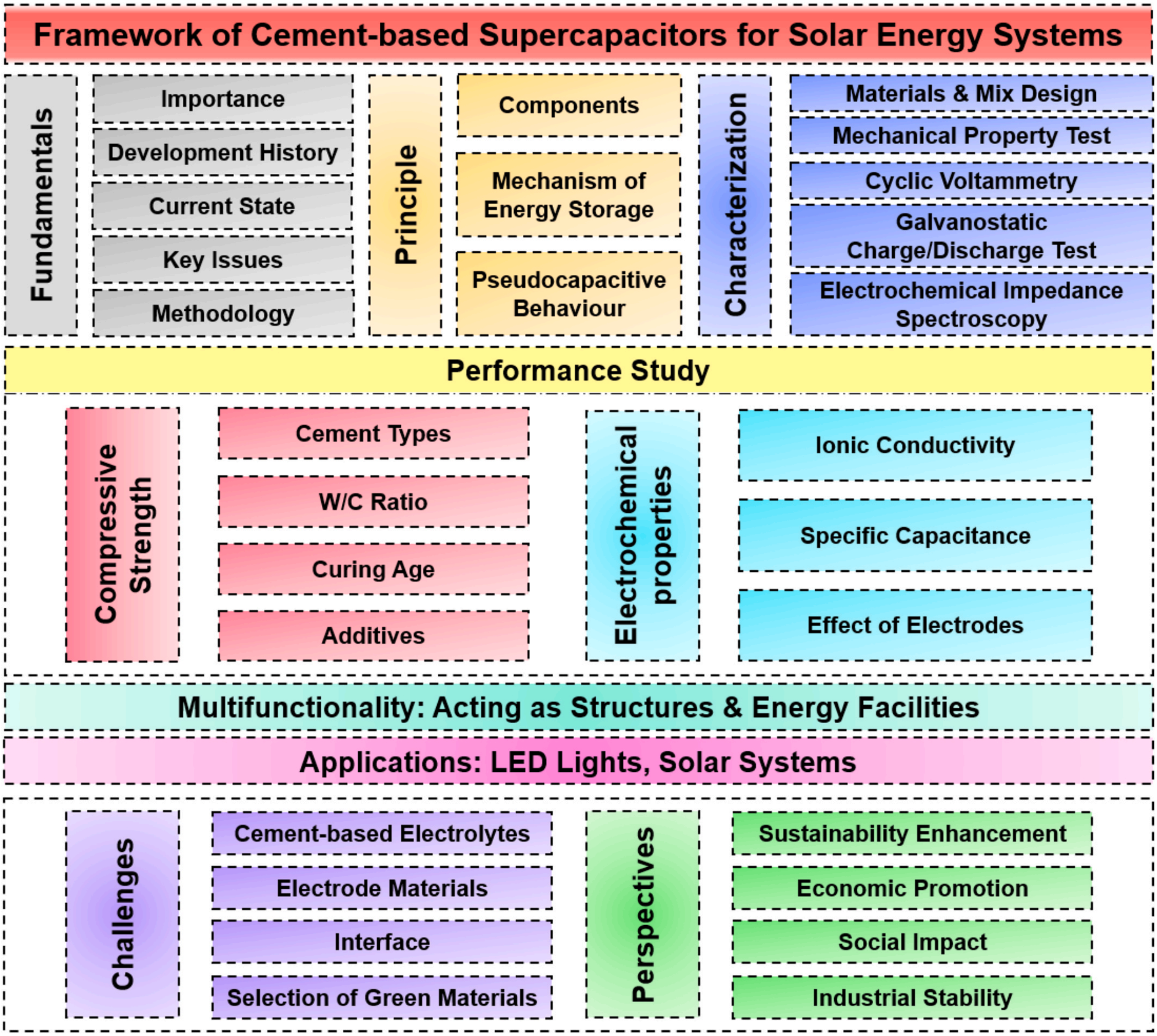

Fig. 3. Framework of the review.

2. Principle concept of CBSC

2.1. CBSC components

The key components of cement-based supercapacitors (CBSC) include the electrodes and the cement-based electrolyte. Electrode materials typically consist of carbon materials, metal oxides, conductive polymers, or composites of these materials. Carbon materials like activated carbon, graphene, and carbon nanotubes are widely used due to their high surface area and excellent electrical conductivity. Metal oxides such as MnO_2 and NiO offer high capacitive properties and are often combined with carbon materials for enhanced performance. Conductive polymers, including polyaniline and polypyrrole, contribute strong electrical conductivity and favorable electrochemical properties. Composite materials enhance performance by combining the beneficial properties of multiple components. In CBSC, these electrode materials are often dispersed or embedded within the cement matrix, creating a composite structure. With careful selection and design of electrode materials, CBSC can achieve superior performance, suitable for a range of energy storage applications.

The electrolyte in CBSC is composed of a cement matrix and electrolyte additives, which are typically materials with high ionic conductivity to facilitate ion transport. The cement matrix serves as the structural backbone, providing mechanical strength and durability to the solid-state supercapacitor. Various additives, such as carbon materials, salts, ionic liquids, or polymer electrolytes, are incorporated to enhance ionic conductivity and stability. Salts create ionic conductive pathways within the cement matrix, supporting electrochemical reactions and charge storage. Ionic liquids, known for their high conductivity and chemical stability, significantly boost the performance of CBSC. Polymers enhance ionic transport and improve stability, optimizing the overall efficiency and cycle life of the device. Through careful selection and proportioning of components, along with refinement of the preparation process, CBSC can achieve high energy density, high power density, and long-term operational stability.

2.2. Energy storage mechanism

Fig. 4 shows the process, mechanism, and energy changes of cement-based supercapacitors. Mixing conductive polymers, inorganic conductive fillers, alkaline solution, and deionized water with cement particles, creates cement-based electrolytes. After a period of curing, a solid electrolyte with conductive pathways can be obtained, as shown in Fig. 4(a). Fig. 4 (b) illustrates the electrode manufacturing process. The composite electrodes are generally made of conductive materials such as metal and carbon nanomaterials, which can combine their advantages to get a better performance of CBSC.

The energy storage mechanism of cement-based supercapacitors is a combination of electrical double-layer (EDL) at the electrolyte–electrode interface, redox reaction in electrodes, and electrolyte charge storage mechanisms [18]. Fig. 4(c) represents 2D and 3D diagrams of the charged state of the supercapacitors, as well as an illustration of the corresponding equivalent circuit. During the charging of CBSC, anions are absorbed on the surface of the anode and cations are adsorbed on the surface of the cathode to balance the charge. These ions are released during discharge. When positive and negative charges are separated, electric double layers (EDL) is formed at the electrode–electrolyte interface to store electrical energy, and this capacitive behavior is referred to as electric double layer capacitors (EDLCs) [19]. Fig. 4(d) is the evolution of voltage and chemical potential across the cement-based electrolyte in contact with an anode and a cathode. When charging, the voltage of the electrodes and the chemical potential of the cation will increase. Meanwhile, a stability window is created to provide enough energy density and guarantee performance.

EDLCs store electrical energy by accumulating electrostatic charges at the interface between the electrodes and the electrolyte [20]. An ion-conductive but electrically insulating electrolyte is used as the medium to allow the movement of ions in the EDLCs. They exhibit higher energy density than conventional capacitors due to their maximum effective surface space [15] and much higher power density than batterie due to double-layer capacitance [21]. The concept of EDLCs was initially proposed and shaped in the 19th century by Helmholtz [22] and it had been modified by Gouy and Chapman and Stern [19,23], as shown in Fig. 5.

The Helmholtz model explained capacitance behavior that opposite charges are layered at the electrode/electrolyte interface and parted by an atomic distance, similar to two-plate, conventional capacitors [15,25], as schematically explained in Fig. 5 (a). Gouy and Chapman modified the Helmholtz model into the diffusive layer model [26,27], where the distribution of ions is sparser and decreases with distance from the electrode. Furthermore, the Helmholtz model and the Gouy-Chapman models were combined by Stern to establish the Stern model in which there are two regions of particle distribution. Fig. 5 (c) shows a diffusive layer and the Stern layer (compact layer). The Stern model represents that a charged adsorption layer is formed on the surface of the electrode, and ions are adsorbed on the electrode surface to form a dense adsorption layer. In contrast, the ions in the diffusive layer are distributed at a lower density. Smaller cations, owing to their higher charge density, typically attract and orient four to six water dipoles through their electric field. The closest position to them is the Outer Helmholtz Plane (OHP). This model gives a more complete understanding of the structure of the double electrical layer.

The capacitance for an EDLC (C_{dl}) originates from the Stern layer capacitance (C_{H}) and the diffusive layer capacitance (C_{diff}). C_{dl} can be demonstrated as Eq. (1):

$$\frac{1}{C_{dl}} = \frac{1}{C_H} + \frac{1}{C_{diff}} \tag{1}$$

The capacitance of a supercapacitor can be expressed as Eq. (2):

$$C = \epsilon_r \varepsilon_0 \frac{A}{d} \tag{2}$$

where ε_0 is the dielectric constant in vacuum; ϵ_r is the relative dielectric constant of a supercapacitor; and A and d are respectively the electrode area and electrode spacing of the supercapacitor.

In cement-based solid supercapacitors, a space charge layer is formed at the electrode–electrolyte interface. Applying a voltage to the capacitor creates a potential difference and redistributes ions and creates interfacial charge transport pathways, storing charges at the electrode–electrolyte interface, as shown in Fig. 6 [11]. In addition, an interfacial layer forms when two materials with different chemical potentials are in contact and/or react. This layer can retard or accelerate ion transport across the interface [11].

2.3. Pseudocapacitive behavior

Unlike traditional capacitors, which store energy through the physical separation of charges, pseudocapacitors store energy through fast faradaic redox reactions occurring at or near the surface of the electrode

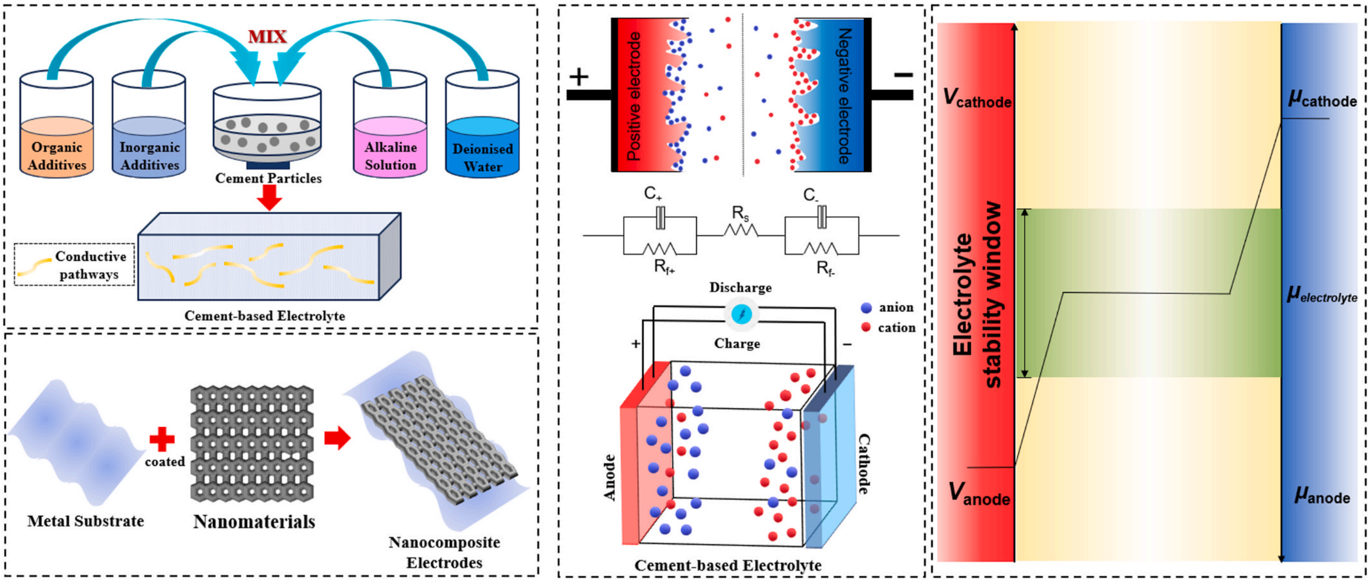

Fig. 4. Schematic diagram of cement-based supercapacitors: (a) electrolyte manufacturing process, (b) electrode manufacturing process, (c) mechanism of cement-based supercapacitors, (d) evolution of voltage and chemical potential, where "+" represents mobile cations [16,17].

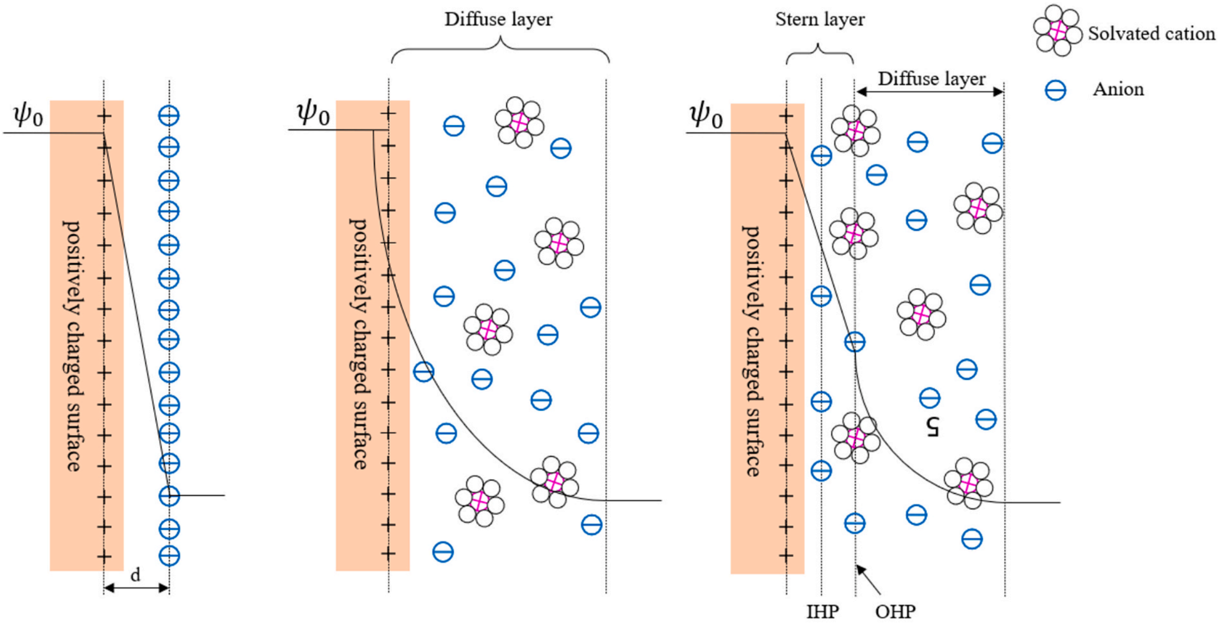

(a) (b) (c)

Fig. 5. Models for the EDL at a positively charged surface: (a) the Helmholtz model, (b) the Gouy-Chapman model, and (c) the Stern model [24].

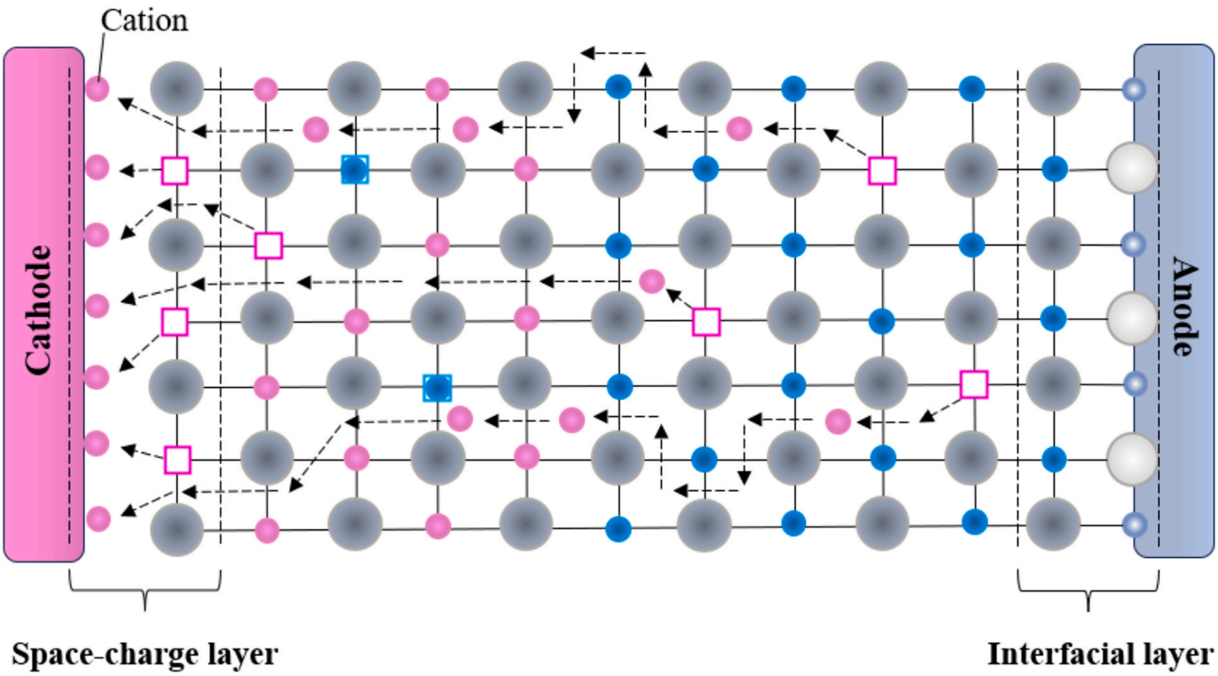

Fig. 6. Cation transport in cement-based electrolytes [11].

material. The selection of pseudocapacitive electrode materials capable of redox reactions is one of the most important ways to improve the electrochemical performance of CBSC [28,29]. Unlike EDLCs, the charge storage mechanism of pseudocapacitive materials is not purely electrostatic but involves Faradic processes – redox reactions [30–33] – that significantly improve properties such as the specific capacitance of CBSC [34]. When a reversible redox reaction takes place at or near the surface of a suitable electrode material, the electrochemical behaviour mirrors that of electric double-layer capacitors (EDLCs). However, the charge storage capacity is greater due to the additional contribution from the redox reactions [35].

Fig. 7 shows the schematic diagrams of three different reversible pseudocapacitor behaviors. The first is underpotential deposition. Underpotential deposition occurs when cations in the electrolyte form an adsorbed monolayer on the surface of a metal electrode with a higher redox potential [31,36]. As shown in Fig. 7 (a), the underpotential deposition of Pb^{2+} on the surface of the Au electrode can provide pseudocapacitance [37].

The second is redox pseudocapacitor [35]. It occurs primarily at the surface of the electrode, and Faraday charge transfer occurs between the electrode and the ions in the solid electrolyte. Fig. 7 (b) shows the redox processes during potential cycling [36,38], which creates much

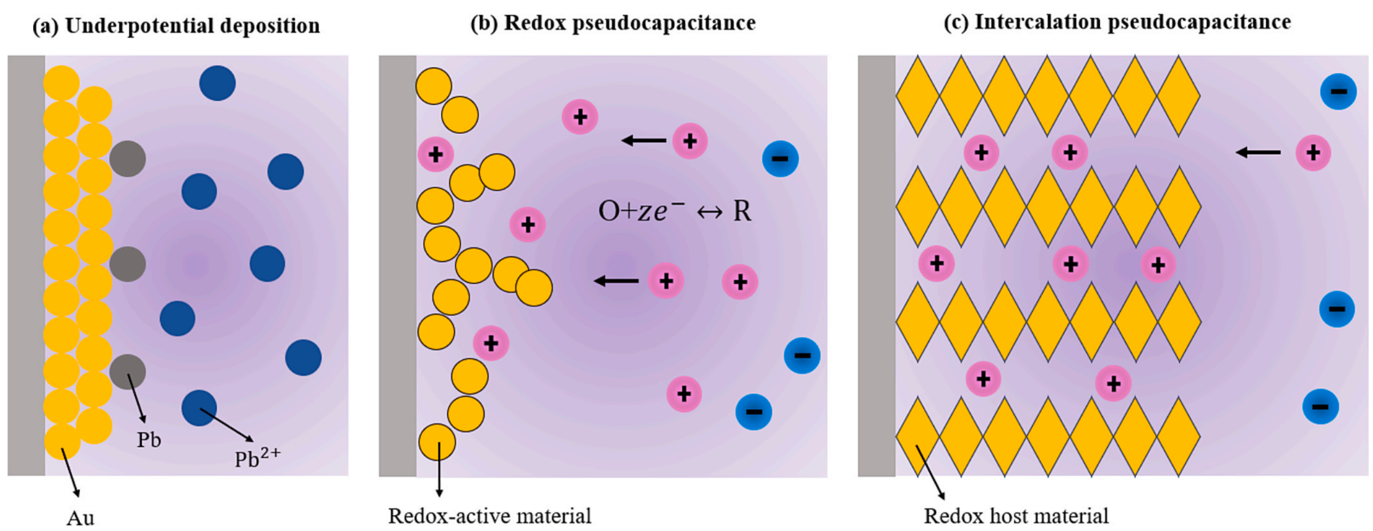

Fig. 7. Three types of reversible pseudocapacitors: (a) Underpotential deposition, (b) redox pseudocapacitance, (c) intercalation pseudocapacitance.

pseudocapacitance and dominates the charging mechanism [32]. The third is intercalation pseudocapacitance. It involves the rapid diffusion of ions into and out of ion-conducting channels or layers within the matrix without the change of crystallographic phase [32]. As a result, the ultra-stable structure is maintained in the electrochemical reactions [36].

Cement-based electrolytes also have energy storage capabilities under certain conditions. During the hydration process, pores of different sizes are formed within the cement and these pores are interconnected to form the pores that can be used for charge transport by ion diffusion [39]. In addition, cement-based electrolytes with redox activity have been developed and can provide excellent energy and power density [18]. Therefore, the efficiency of energy storage can be further improved by adding appropriate additives, such as metal oxides. Overall, CBSC consists of multiple capacitive behaviors with different energy storage mechanisms. Their design and application have been demonstrated to be feasible, by proper selection of electrodes and electrolytes.

3. Characterization of CBSC

The performance of CBSC can be evaluated from two different aspects: the traditional mechanical properties, and electric and electrochemical properties [40]. Table 1 displays a technique to evaluate the compressive strength of CBSC, and three techniques to evaluate the electrochemical properties of CBSC. Compressive strength is an important indicator of cement-based materials, which is the basis for realizing the multifunctionality of composites. Generally, the cube compressive strength test has been used to measure the compressive strength of the specimens in the laboratory. Cyclic voltammetry (CV) can be used to measure current at a fixed sweep rate, while galvanostatic charge/discharge (GCD) measures the voltage of a device at different currents. Electrochemical impedance spectroscopy (EIS) can control both current and voltage, so either voltage or current can be measured to collect the impedance data. Compared to CV and GCD, EIS imposes a smaller excitation signal, resulting in a more linear current–voltage characteristic. In addition, EIS can be used to characterize charge transfer, mass transport, and charge storage mechanisms, as well as to estimate energy and power properties [40–42]. However, it is important to note that the equivalent resistance derived from the EIS test is typically much smaller than that derived from the GCD test [43], and therefore needs to be thoroughly evaluated when characterizing supercapacitor performance.

Table 1
Advantages and disadvantages of different characterization techniques.

Technique	Advantages	Disadvantages	Refs.
Compressive strength test	Intuitive resultsHigh precision	Cannot represent the strength of the entire structure	[44]
CV	Specific capacitanceDifference between EDLC and PC	Thermodynamic aspect is ignored	[45–47]
GCD	CapacitanceDifference between EDLC and PC	The difference between electric double layer materials is not obvious	[46,47]
EIS	Different resistances Specific capacitanceDegradation behavior	Only evaluation at low voltage	[46,48,49]

3.1. Materials and mix proportions

The main components of a supercapacitor are electrolyte, electrodes and separator. In CBSC, the cement matrix is electrolyte, while it also can act as the separator due to its insulation. CBSC combines a low-cost cement matrix with high-performance conductive materials. Materials include different types of cement, carbon materials and conducting polymers, and use ionic liquids or organic electrolytes to provide ion-conducting pathways. Although some conductive materials like CNTs and graphene are relatively costly, their excellent conductivity and high specific surface area significantly enhance the energy density and power density of supercapacitors. By optimizing material ratios and refining production processes, cement-based supercapacitors can achieve high performance at a significantly reduced overall cost, presenting a broad spectrum of application prospects. Table 2 shows the configuration of potential materials for CBSC, including electrolyte type, composition and preparation of electrodes and their contribution.

3.2. Compressive strength testing

In the laboratory, compressive strength is mainly tested using the cube compressive strength test, which is a standard and specialized method [65,66]. After the cement specimens are prepared and cured for 28 days, they are subjected to a compression test using a compression tester or universal testing machine. When pressurizing, the load shall be applied continuously and uniformly, and the pressurization rate shall be adjusted according to the expected strength of the specimen. When the specimen is close to destruction and pole deformation begins to occur, it is necessary to stop adjusting the machine pressure until it is destroyed

Table 2
The configuration of potential materials for different CBSC components.

Electrolyte type	Electrode composition	Preparation method	Contribution	Refs.
—	LiC_6	Intercalation or electroplating method	Ion transport rate can be faster and voltage penalty can be small	[50,51]
—	Na_xC_6 and Li_xC_6	Intercalation method	The reversible capacitance can be stable	[52,53]
Argyrodite Li_6PS_5Cl	$LiCoO_2$, $LiNi_{1/3}Co_{1/3}MnO_{1/3}O_2$, and $LiMn_2O_4$	Solid-state reaction method and co-precipitation method	The compatibility and capacity retention are good	[54]
—	NCM oxides	Co-precipitation method	High energy density and operating voltage can be provided	[55,56]
Portland cement/ PAA	rGO, MnO_2 and rGO/ MnO_2	Hydrothermal synthesis method	Long-term stability is good	[57]
Portland cement/ PAM	rGO/SnO_2	Ultrasonic dispersion method and hydrothermal synthesis method	The diffusion of ions is facilitated, and active surface area is increased	[58]
MPC/PAM	rGO/Ni foam	Hydrothermal synthesis method	Energy density and power density are both improved	[59]
Portland cement/ PAM with Na_2SO_4	PPy-NTs and CNTs	Self-polymerization method	Conductivity and capacitance are high	[60]
Portland cement/ PAA	rGO/Ni_xCo_yS (Ni:Co ratio is 1:0, 0:1, 1:2, 2:1) and rGO/ Fe_2O_3	Hydrothermal synthesis method	Ion access and charge transfer are fast, and areal capacitance and its retention are increased	[61]
LLZO	—	Solid-state reaction method	Operate dendrite free at sufficiently high current densities	[62]
NASICON	—	Solid-state reaction method	Excellent thermal stability and environmental friendliness are provided	[63,64]

and record the destructive load. Compressive strength is expressed in Newtons per cubic millimeter (MPa) as defined in Eq. (3):

$$R_C = \frac{F_C}{A} \tag{3}$$

where R_C is compressive strength of the specimen (MPa) , F_C is maximum load at destruction of the specimen (N) and A is compressive area of the specimen (mm^2).

3.3. Cyclic voltammetry

CV testing applies a linearly changed electric potential between positive and negative electrodes for two-electrode systems, or between reference and working electrodes for three-electrode configurations [40]. A positive voltage sweep charge achieves the maximum voltage; the reverse sweep charge is immediately applied [15]. The speed of potential change (mV/s) is called the scan rate, and the range of potential change is called the potential window or operating potential [23]. Fig. 8 demonstrates the characteristic cyclic voltammograms (CVs) of three electrolytes at a scan rate of 5 mV/s.

CV can also be used in practice to determine the potential window or operating voltage of supercapacitor materials, and to study the reversibility of charging and discharging processes [68,69]. In addition, the capacitance and other electrochemical properties of the material can be obtained by integrating the CV curves. In particular, the capacitance can be calculated based on the Eq. (4) [40,70–72]:

$$C_T = \frac{\Delta Q}{\Delta V} \tag{4}$$

where C_T is the total capacitance of a supercapacitor, ΔQ is the CV curve integral area, which is also the total charge and ΔV is the change of a given voltage.

$$C_T = \frac{\Delta Q}{\Delta V} = \frac{\int_0^{2V_0/V} |i| dt}{2V_0} \tag{5}$$

where V_0 represents the given voltage at a specific time; $|i|$ represents the absolute value of current; and dt is differentiated with respect to time.

$$C_S = \frac{C_T}{\varphi} \tag{6}$$

where C_S is the specific capacitance of a supercapacitor; and φ is related to many aspects of the electrode material, including the mass, volume, surface area, etc. After we get the value of capacitance C_T, the corresponding C_S can be calculated by Eq. (6). In addition to φ, there are some other factors that can influence the value of C_S dramatically [73–75], such as experimental conditions, mass loading and the properties of electrodes.

3.4. Galvanostatic charge/discharge test

Galvanostatic charge/discharge (GCD) is the most versatile and accurate method to characterize the supercapacitors. It is conducted by repeatedly charging and discharging the working electrode at a constant current level [40], to evaluate the capacitance, energy density, power density and peak current. Meanwhile, it can also be used to investigate parameters such as cycling stability. The overall GCD measurement process involves two steps: first, supercapacitors charge via a constant current, and second, it is discharged in a specific time or voltage range [15]. Therefore, Eq. (7) can be used to calculate the capacitance [40]:

$$C_T = \frac{I \Delta t}{\Delta V} \tag{7}$$

where I is the galvanostatic current and Δt is the charging/discharging time under a given potential change ΔV. In turn, Eq. (8) is obtained:

$$C_T = \frac{I_{dis} \Delta t_{V_0 - 2V_0}}{V_0} \tag{8}$$

where I_{dis} is the discharging current and Δt is the time difference between two given operating windows (V_0 and $2V_0$). The time–voltage in GCD test is presented in Fig. 9.

3.5. Electrochemical impedance spectroscopy

Electrochemical impedance spectroscopy (EIS) is an electrochemical analytical method based on an alternating current measurement technique. The impedance of a supercapacitor as a relationship of frequency (e.g., from 0.01 to 100 kHz) by applying alternating potential at a low amplitude (e.g., ±5 to ± 10 mV) superimposed on a steady-state voltage [15]. The calculation results of capacitance can be expressed in a Bode plot to explain the response between the frequency and the phase [40], and the imaginary parts $Z(f)''$ and real parts $Z(f)'$ of the supercapacitor impedances on a complex plane are shown in a Nyquist plot [76–79].

Fig. 10 represents the ideal Nyquist plots. From Fig. 10 (a) there is a straight line [80], which represents the capacitance as a constant over the frequency range. Fig. 10 (b) shows the ideal pseudocapacitive

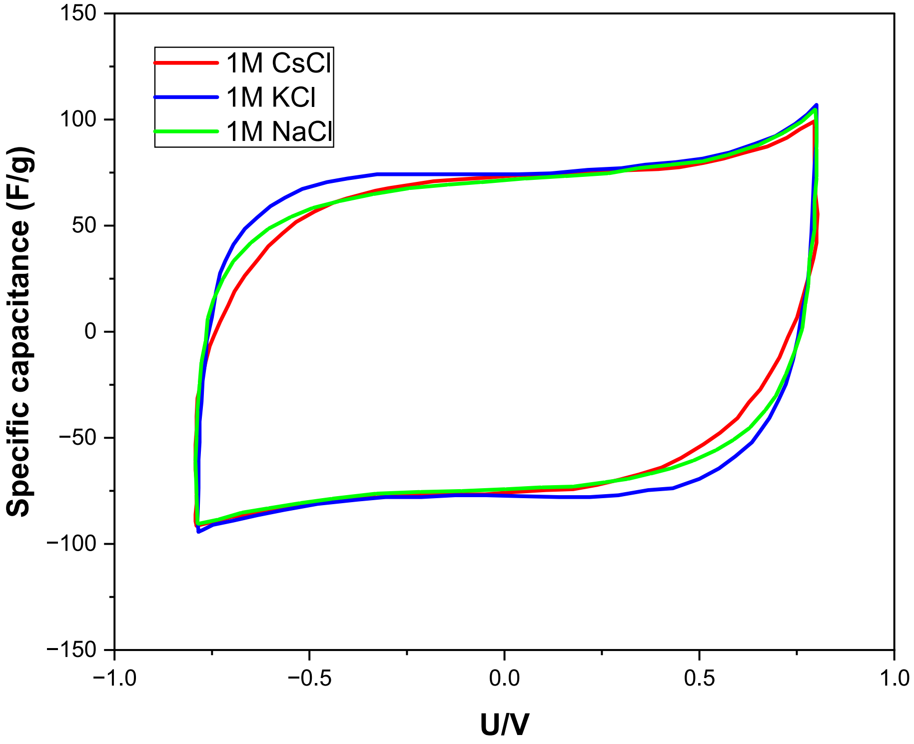

Fig. 8. CVs of the in-situ measurements using a scan rate of 5 mV/s [67].

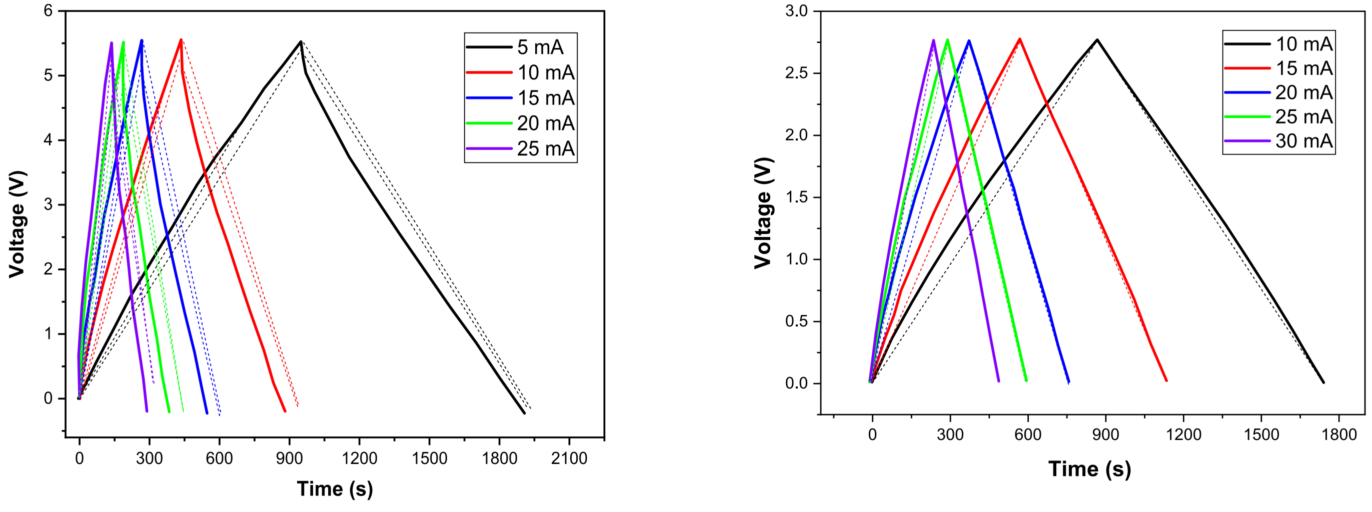

(a) EDLCs

(b) Pseudocapacitors

Fig. 9. Time-voltage in GCD test [70].

electrochemical impedance response. The semicircular region refers to the high frequency region and is associated with charge transfer impedance and double layer capacitance. The low frequency vertical line is related to the charge stored by the electrochemical reaction. The capacitance can be expressed by Eq. (8).

$$C_P = \frac{zF}{RT} \bullet \frac{\theta(1-\theta)}{g\theta(1-\theta)-1} \tag{8}$$

where θ is the electrochemically active point covering the saturation level, g is an exclusion factor, which is negative for repulsion between each locus and positive for the opposite.

4. Performance study of CBSC

4.1. Effects on compressive strength

Cement is one of the most widely used materials globally, with estimated production reaching 4.1 billion tons in 2022. It plays a crucial role in meeting the global demand for housing and infrastructure [82]. In many developed countries, buildings account for a significant portion of total energy consumption [83,84]. As a result, a key future trend in construction is the development of building materials with energy storage capabilities, along with their integration into renewable energy systems.

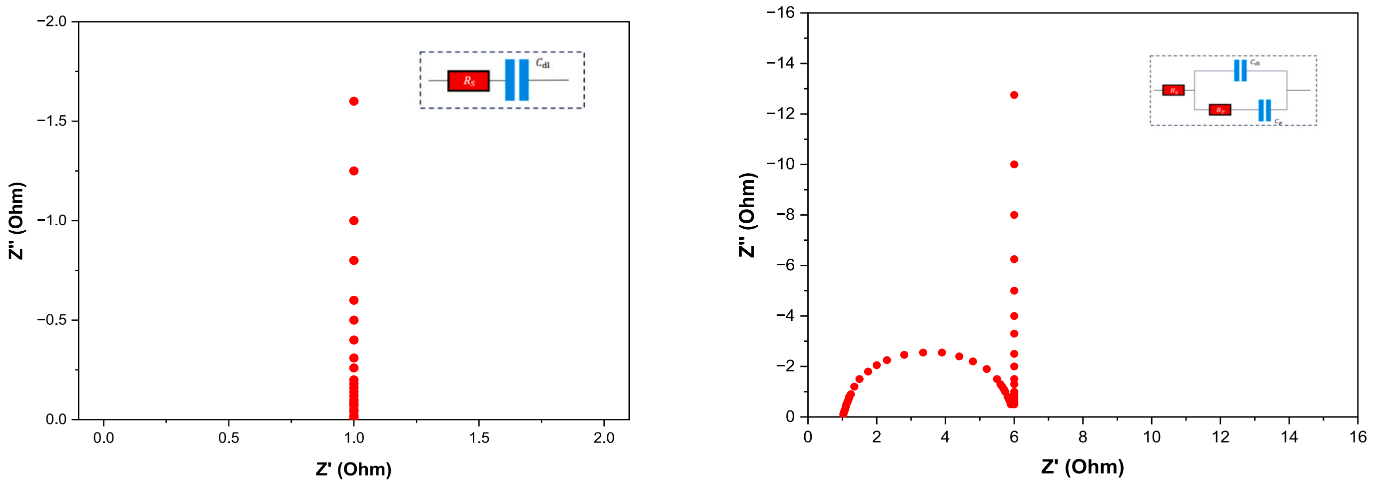

(a) EDLCs

(b) Pseudocapacitors

Fig. 10. Nyquist plots of ideal supercapacitors [81].

4.1.1. *Effect of cement type*

Different types of cement have been used to produce CBSC. Differences in ion types, ion concentrations in the pore solution, and pore connectivity influence the resulting electrolytes, affecting both their mechanical and electrochemical properties. Zhang et al. [10] made a novel structural supercapacitor using an ordinary Portland cement (OPC) paste and found that there is no pseudocapacitive effect in the supercapacitor, while an ideal double layer mechanism was possessed by the supercapacitor.

In addition to OPC, eco-cement-based materials have also been used to fabricate cement-based solid electrolytes. Ma and Zhang [85] chose magnesium phosphate cement to make structural supercapacitors due to its high early strength, good chemical resistance, and higher porosity. The results showed a significant increase in both the compressive

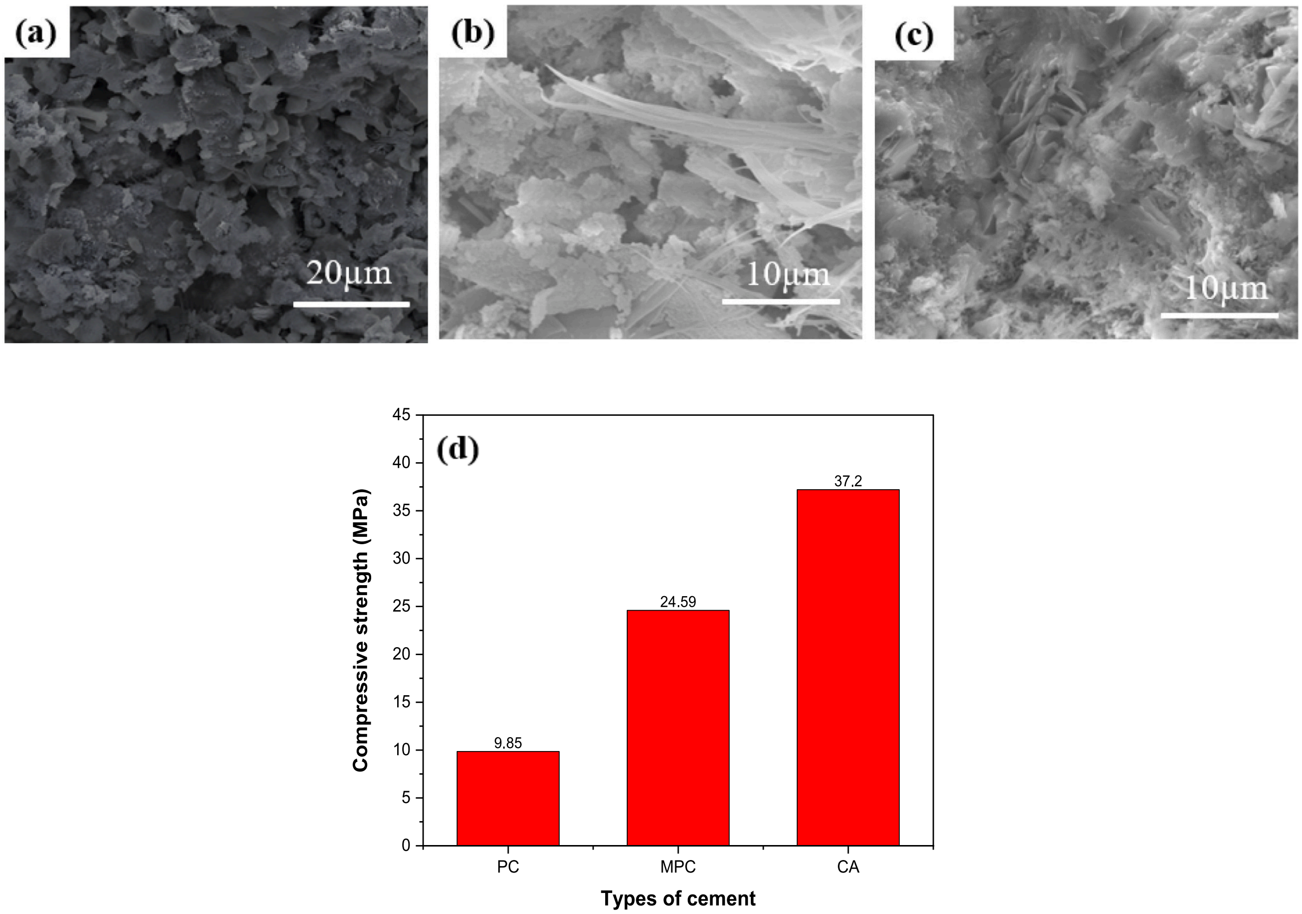

Fig. 11. Comparison of microstructure and effect of cement types on compressive strength: (a) SEM of PC [10], (b) SEM of MPC [85], (c) SEM of CA [87], (d) Effects of three types of cement.

strength of the material after 28 days and the specific capacitance. Tu et al. [86] mixed aluminate cement with polyacrylic acid to produce structured electrolytes. Their compressive strength was further improved, and they exhibited better electrochemical properties due to the use of more advanced electrodes. These comparisons illustrated the significant role played by different types of cement in various aspects of performance, as shown in Fig. 11. The specific capacitance and compressive strength of OPC-, MPC- and CA-based electrolytes increased, which could be attributed to the increase in stored energy due to more ions in MPC and CA. Meanwhile, MPC and CA had relatively high early strength, which undoubtedly increased the compressive strength. By comparing Fig. 11 (a) to Fig. 11 (b), the OPC specimens exhibit a loose structure with more pores, making the connections between the particles weaker, while the MPC specimens have a mixed structure of flakes and fibers, which is denser and enhances the compressive strength. The CA specimens show a finer and more complex fibrous structure. These tightly interwoven structures form a denser mesh skeleton structure and reduce the porosity, which allows the material to disperse stress when under pressure, further improving their overall compressive strength. Table 3 shows the comparison of different cement types between microstructure and advantages.

4.1.2. *Effect of water-to-cement ratio*

The effects of water-to-cement (W/C) ratio and curing age should also be considered. As the W/C ratio increases, the porosity of the cementitious material increases, resulting in a sufficient number of interconnected channels or pores for the transport of ions within the pores. However, a high W/C ratio will result in a reduction in strength. Therefore, the selection of a suitable W/C ratio according to the actual requirements is essential to obtain the best mechanical and electrochemical properties. Zhang et al. [10] investigated the effect of different W/C ratios on the multifunctionality of cement-based supercapacitors and found that a W/C ratio of 0.3 gave the most optimal specific capacitance. Chanut et al. [39] also concluded that the ideal W/C ratio should not be too high and that 0.42 was the most appropriate value by measuring the capacitance of three different W/C ratios at different high scan rates. Both results demonstrate a similar trend. Specifically, high water-cement ratios result in larger hydrated pores and lead to higher capacitance values. However, while these higher ratios enhance capacitance, they also weaken the material's strength. This is due to increased hydration porosity, which causes stress concentrations around the micrometer-sized pores.

4.1.3. *Effect of curing age*

The effect of curing age on the capacitance of CBSC is shown in Fig. 12. The relationship between compressive strength and specific capacitance of different types of cement at different curing times is compared. It shows a positive correlation between the compressive strength of the three cementitious composites and the curing time. Chanut et al. in their study of carbon cement-based supercapacitors demonstrated that the capacitance is independent of the experimental conditions and is independent of the test conditions through a combination of Boltzmann's integrodifferential equations and the theory of viscoelasticity of solids [39]. Therefore, we believe that the capacitance of cement-based materials and their related properties are only associated with the inherent properties of the material itself, such as specific surface area, porosity, etc.

Table 3

The comparison of different cement types.

Cement type	Corresponding microstructure	Advantages	Refs.
OPC	Continuous monolithic structure and agglomeration of nanoparticles	Ion storage, ion movement and mechanical bearing capacity can be impacted positively	[101]
MPC	Porous structure	Enough channels for ion transport are provided	[85]
CA	Plate-like crystal structure	Mechanical properties can be enhanced	[87]

4.1.4. *Effect of additives*

The most used cement additives for CBCS today are polymers, most of which include polyethylene oxide (PEO), polyvinyl alcohol (PVA), polyacrylic acid (PAA), potassium polyacrylate (PAAK), polyacrylamide (PAM) and polyethylene glycol (PEG) [88]. These polymers are generally believed to interact with cement hydration both physically and chemically, influencing the properties of the hydration products. The two interactions have beneficial effects on the microstructure and macroscopic properties of polymer-modified cements [89], resulting in the formation of a denser and more complete microstructure within the material [90]. During the preparation process, the polymer solution is usually mixed with cement. In this process, the polymers, cement hydration products and ions are cross-linked [91,92], while the polymer solution can optimize the pore distribution of the cement matrix and fill the pores between unreacted cement particles, significantly improving the mechanical properties of the polymer-modified cement [93,94]. According to the request regarding mechanical and electrochemical performance, PAM is the best suited to meet the balance of these two criteria, which is discussed in this section.

Fig. 13 shows the microstructure of several different polymer-modified cements and their effect on the compressive strength of CBSC. The interconnected pore structure can be identified clearly after adding PVA to cement, as shown in Fig. 13 (a).The microstructure of PVA in harden cement paste presents a strip shape and shows the characteristics of a smooth surface [95]. A bicontinuous microstructure consisting of PVA and OPC is formed after PVA penetrated through the pore structure [96]. Fig. 13 (b) shows that the PAM is well distributed in the hardened cement pastes and becomes a whole. The hardened cement paste is encapsulated by the PAM and dispersed in the matrix in granular form. According to the SEM results, the PAM and hardened cement can achieve close integration by synchronous reaction method and like PVA, the addition of PAM can also form a bicontinuous microstructure [97,98]. The cement/polymer composite material with low 5 % PAA has a finer and denser porous structure depending on the cross-linking networks of PAA interconnected with C-S-H. After the content of PAA increases, more mesoporous pores and some harmful macropores are formed as shown in Fig. 13 (c), which lose the microstructure of the composite [97–99]. Fig. 13 (d) compares the microstructure of three contents of PEO/OPC. When the content is low, the microstructure is denser, but various pore structures are blocked by the PEO. The polymer particles concentrate and gradually interconnect with each other in the cement electrolyte as the content of PEO increases. These findings prove that a proper polymer content can achieve well-distributed interconnected microstructure between organic and inorganic phases [100]. To ensure good polymer distribution in a water-cement-based supercapacitor, employ high-shear mixing, ultrasonication, pre-dissolve the polymer in a solvent, add surfactants and dispersing agents, use plasticizers, optimize mixing time and speed, control temperature, utilize mechanical homogenizers, and verify with microscopic analysis to achieve uniform dispersion and improved performance.

Fig. 14 shows the XRD patterns of CBSC with two different polymers. The main hydrated products of polymer modified cement electrolytes are $Ca(OH)_2$, Aft and hydrated calcium silicate (C-S-H). The weak diffraction peaks around 26.1° and 42.2° attribute to PAM, while the weak diffraction peaks around 22.3° and 28.9° belong to PEO. This demonstrates that the polymers can bond well with cement matrix during hydration and does not change the type of products. Meanwhile, cement paste, polymers and other metal salts can be used together based on the XRD results. Therefore, cement-based electrolytes modified by polymers are proved to be feasible.

Fig. 15 shows the effect of polymer types and content on the

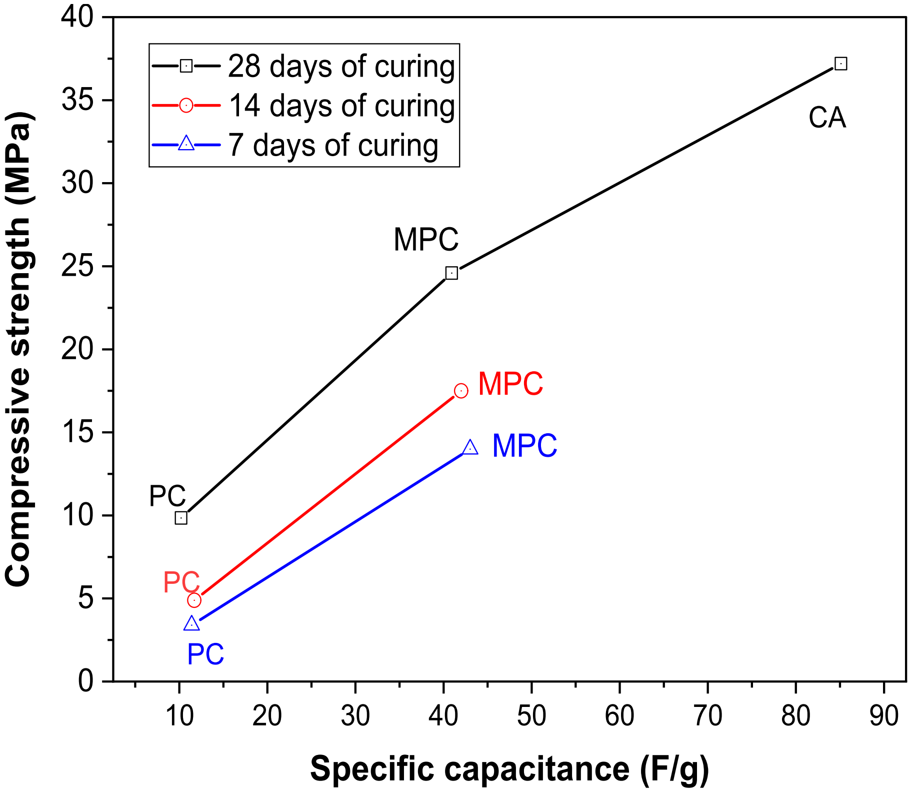

Fig. 12. Relationship between compressive strength and specific capacitance of different types of cement at various curing times [10,85,86].

compressive strength of CBSC. The compressive strength of plain cement paste, for instance, without additives, is generally higher. For PVA, compressive strength is highest at about 2 %. When the level is not less than 4 %, the compressive strength decreases extremely. In the case of PEO, its addition does not increase the compressive strength. Only 2 % of PEO reduces the compressive strength by about 37.5 %. Therefore, PEO should be carefully selected in future studies. The optimum PAA content is between 5 % and 6 %. After that, the compressive strength decreases significantly as the PAA content increases. When the content exceeds 10 %, the compressive strength value begins to fall below 10 MPa and mechanical properties are gradually lost. PAM is a better additive because its addition increases the compressive strength of cement composites and the influence of PAM on compressive strength has certain rules, which is an increase followed by a decrease. However, the study used synchronous reaction method (SRM) [98] which breaks the limitation of the polymer content in the solid electrolyte, thus improving the multifunctionality of the material.

Notably, the preparation of polymer/cement composite solid electrolytes involves the synchronization of hydration reaction and polymerization reaction [105,106]. Polymers interact with cement through both physical and chemical mechanisms, significantly enhancing the properties of cement composites. Physically, polymers aid in the dispersion and distribution of cement particles, fill pores, reduce porosity, and increase density. Chemically, polymers bond with hydration products, such as calcium silicate hydrate, through hydrogen bonding and electrostatic interactions. This optimizes the interfacial transition zone and promotes nucleation and growth. Additionally, polymers enhance the water retention capacity of cement slurries, ensuring adequate hydration. They form a continuous film during the drying process, which improves the mechanical strength and durability of composite materials. These combined effects result in cement-based supercapacitors with excellent electrochemical performance and structural stability. Therefore, the composite particle bonded together tightly, resulting in the increase in the compressive strength [97]. Table 4 gives the advantages and disadvantages of polymer types on cement.

Other conductive materials, such as nanocarbon black, carbon fiber [115] and graphene [116], can be mixed with water and cement. Chanut et al. [39] exploited the synergistic interaction between hydrophilic cement and hydrophobic carbon black between the hydration to create a solid electrolyte with an electron-conductive network for chargeability, storage pores for adsorption of opposite charges, and reservoir porosity for charge transfer by ion diffusion. They visualized for the first time the texture of the carbon network in an electrode and performed spatial correlation analysis of the low- and high-density carbon phases in this network. Charge transfer from the electrolyte to the storage pores of the carbon particles was demonstrated. The intensive nature of the carbon-cement material, i.e., the energy storage capacity per unit volume or mass, was also demonstrated by a quantitative analysis of the energy storage limit states. It is further confirmed that the carbon-cement composite design was scalable in terms of energy storage and could provide sufficient energy storage space for the structure by scaling the material mass to realize the transition from fossil to renewable energy sources.

4.2. Effects on electrochemical properties

Cement-based electrolytes function as structural electrolytes, with cement serving as the primary supporting material [9]. Consequently, the properties of cement significantly influence the performance of these electrolytes, particularly in terms of mechanical strength, as extensively documented. However, electrochemical properties are equally critical, and prior research has highlighted a complex and often contradictory relationship between the mechanical strength of structured electrolytes and their electrochemical performance. Given cement's inherent insulating nature, achieving efficient charge transfer and storage requires careful consideration of factors such as cement type, aggregate, water-cement ratio, additives, and pore solution. The pore solution must

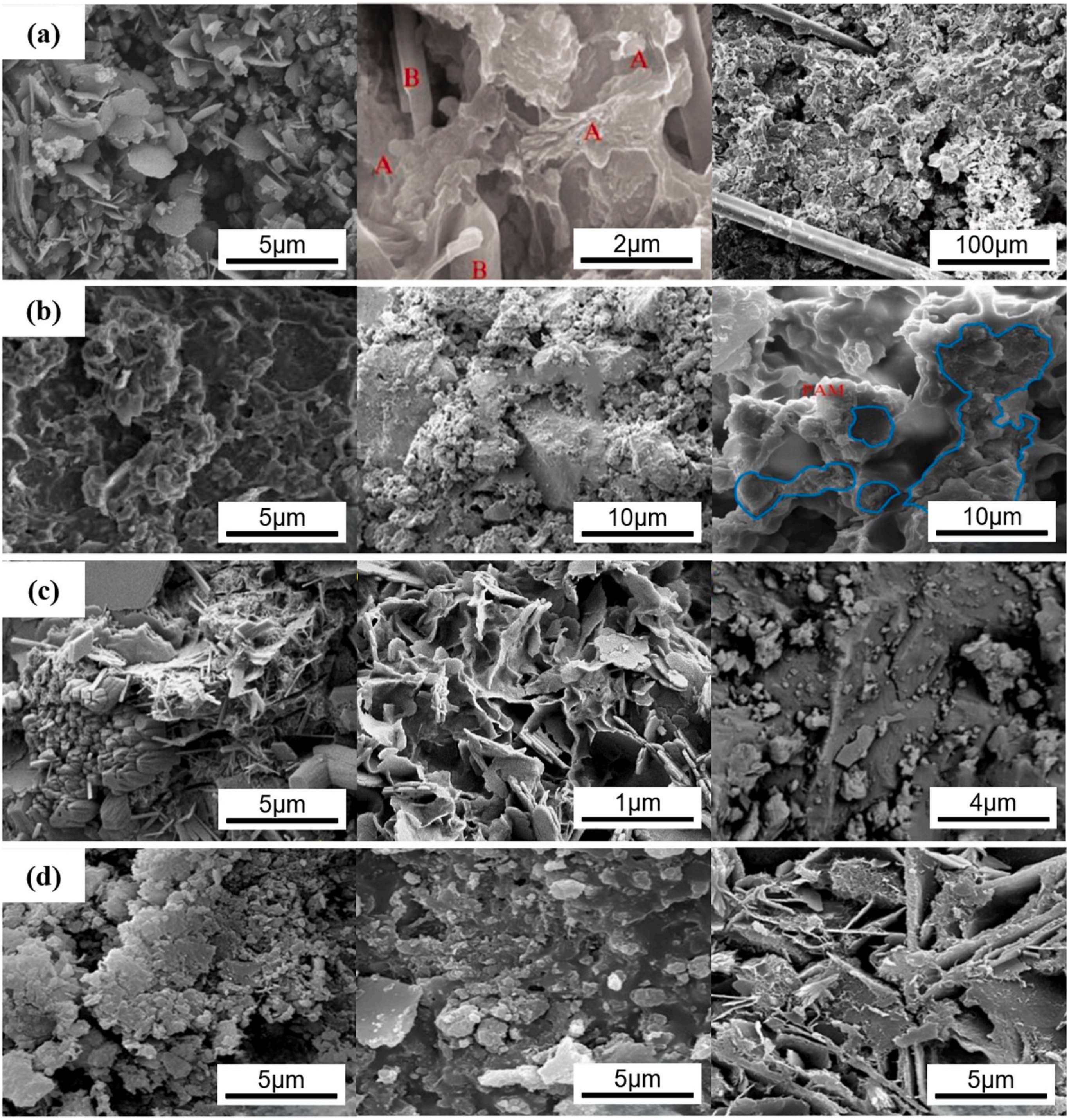

Fig. 13. The SEM of cement/polymer electrolyte (a) 5%, 3% and 25% PVA/OPC, (b) 10% and 30% PAM/OPC, (c) 5% and 30% PAA/OPC, (d) 0%, 2% and 10% PEO/OPC [96–98,100–104].

have an appropriate concentration and be compatible with cement-based materials. Together, these elements profoundly shape the overall electrochemical performance of cement-based electrolytes.

4.2.1. *Effects of conductivity*

Many studies have explored the development of solid electrolytes prepared from inorganic ionic solutions and polymers with higher ionic conductivity [88,117–121]. Cement, on the other hand, in its slurry prior to hydration, can be viewed as a solution containing ions. By modifying the cement with polymer, the compressive strength of the cementitious material can be improved, as well as the enhanced ionic conductivity and anti-leakage of the cement-based electrolyte [96].

Figs. 16 (a) to (d) give the EIS curves of different polymer modified cement-based electrolytes. Fig. 16 (a) compares the EIS curve of 5 types of PAA content. As the PAA content increases from 5 % to 30 %, the internal resistance decreases from 160 to 57 Ω obviously. A porous network structure which provides ions with fast transport paths may be established by a higher PAA content. In Fig. 16 (b), the EIS curve of the same PEO content with two inorganic compounds is shown. The internal resistance of the electrolyte containing LiOTf is higher than another one containing KOH because the former one cannot provide enough mobile ions like the latter (K^+), resulting in poorer conductivity and higher

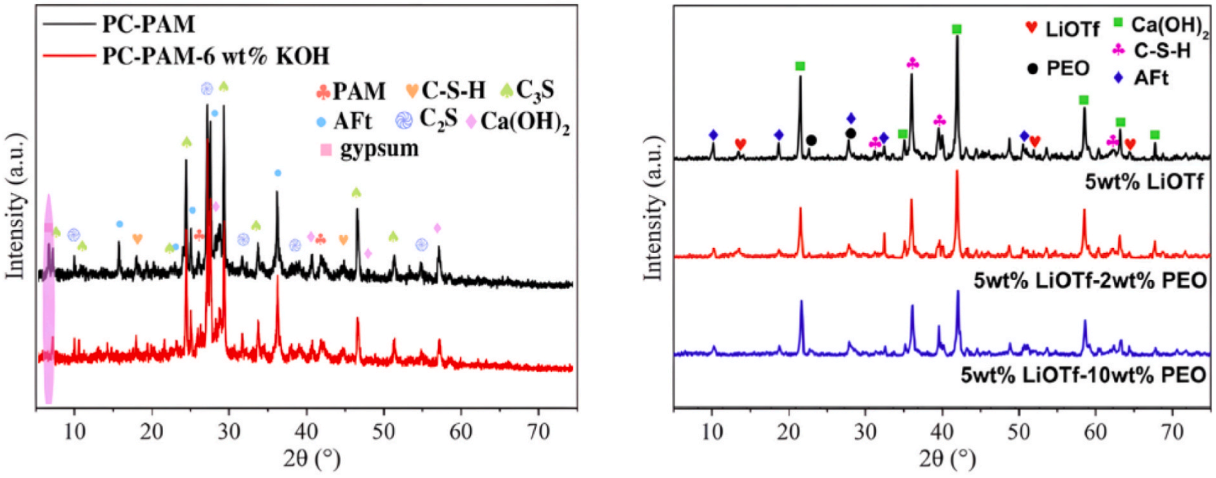

(a) OPC/PAM

(b) OPC/PEO

Fig. 14. XRD patterns of cement-based electrolytes [97,100].

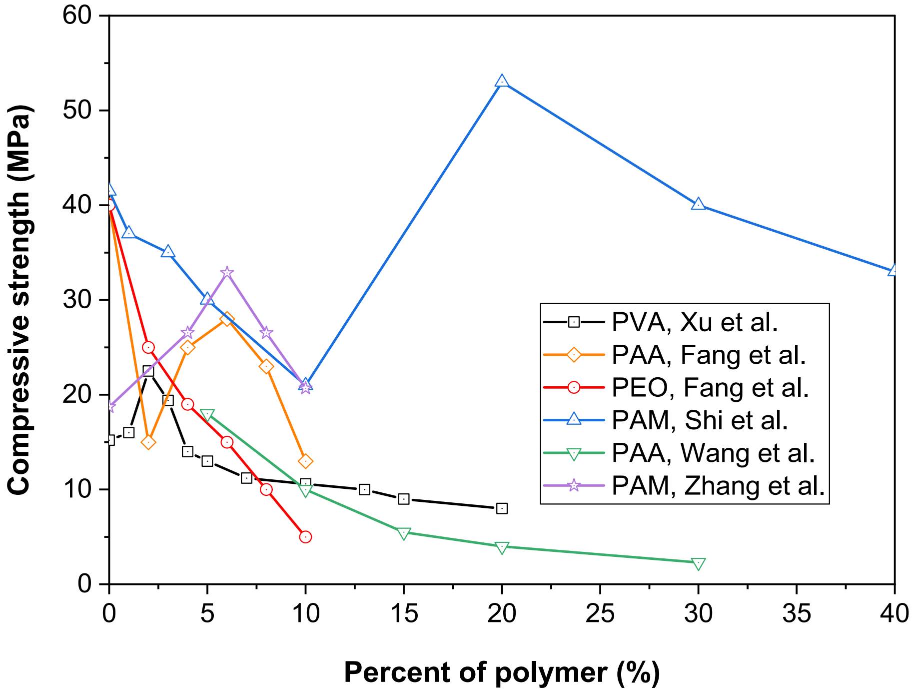

Fig. 15. Effect of polymer types and content on compressive strength [96–98,100,101,104].

Table 4
Influence of polymers on cement-based supercapacitors performance.

Polymer types	Advantages	Disadvantages	Refs.
PVA	Improved durabilityMake the microstructure denser	Increased air void content	[107–109]
PAA	Higher compressive strengthStrengthen local structure	Reduced setting time	[110]
PAM	Higher flexural strengthCreate PAM-cement network	Delayed hydration process	[111,112]
PEO	Hydration products well-distributedDenser microstructure	Reduced flowability	[113,114]

resistance. However, LiOTf exhibits high ionic conductivity and stability, enabling the release of Li^+ and OTf^- ions upon dissolution. This property significantly enhances overall ionic conductivity of the electrolyte, while KOH offers exceptional ionic conductivity, facilitating efficient charge transfer and reaction processes. Fig. 16 (c) and (d) give the EIS curves of different cement-based electrolytes with the same polymer (PAM). It is obvious that the internal resistance of OPC-based electrolytes is much higher than that of MPC-based electrolytes based on the intercept on the x-axis. In addition, no matter what type of cement, the internal resistance decreases, which illustrates the ionic conductivity is promoted by high dosage of PAM in the cement. Notably, the percentage of different contents of PAM/cement is not limited to 40 %. The addition of multiple polymers simultaneously to improve ionic conductivity can also be achieved.

Fig. 16 (e) compares the effect of several different additives on

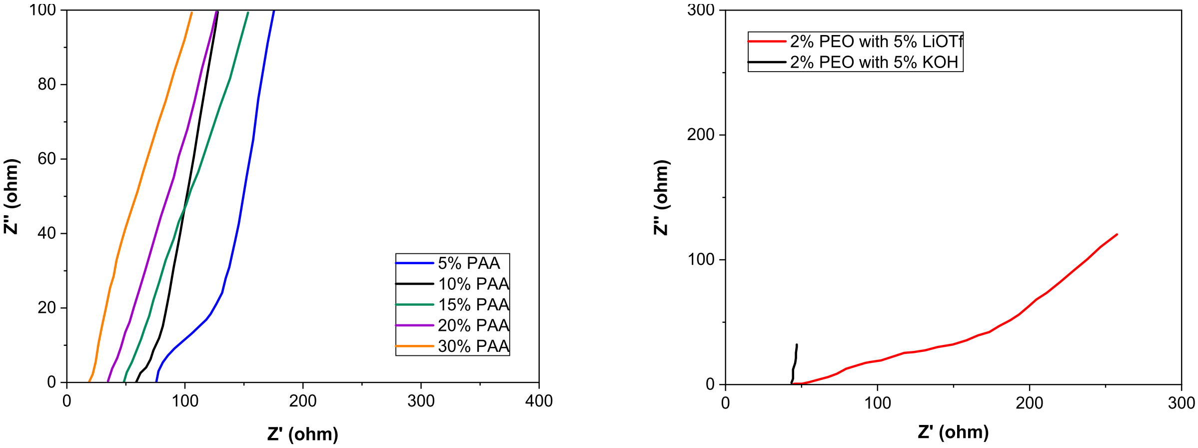

(a) EIS curves of different contents of PAA/OPC

(b) EIS curves of two inorganic compound

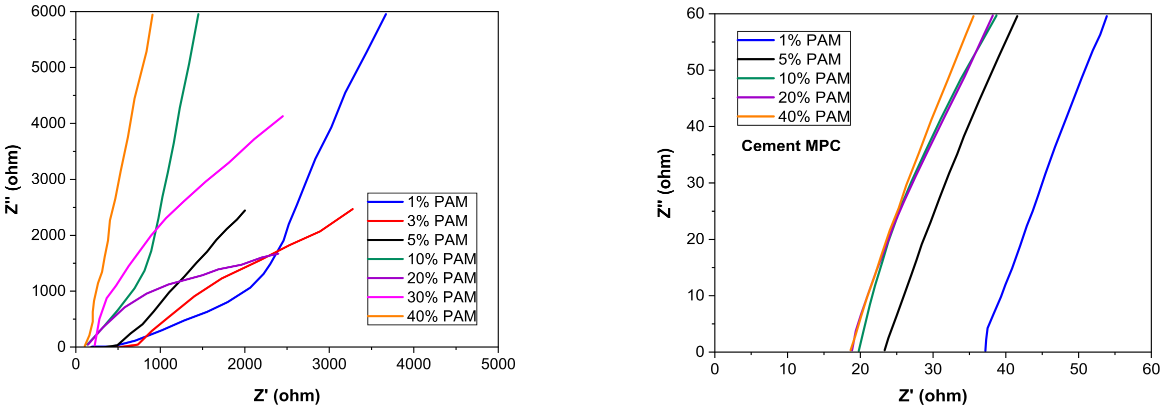

(c) EIS curves of different contents of PAM/OPC

(d) EIS curves of different contents of PAM/MPC

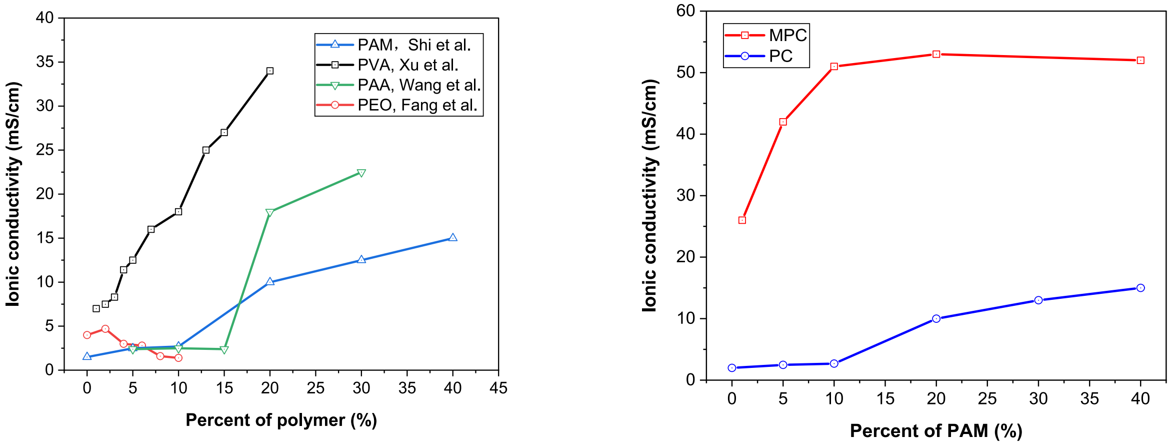

(e) Different polymer contents

(f) Different PAM content on PC- and MPC-based electrolytes

Fig. 16. Effect of polymer types and content on internal resistance and conductivity of cement-based electrolyte [59,96,98,100,104].

electrolyte conductivity at various levels. As can be seen from the figure, except for PEO, the conductivity of the cement-based electrolytes increases with increasing polymer content, and there is an abrupt increase in conductivity when the content exceeds 10 % or 15 %. The reason is likely due to the generated dense, complete, and interconnected conductive polymer network within the cement to reduce the limitations

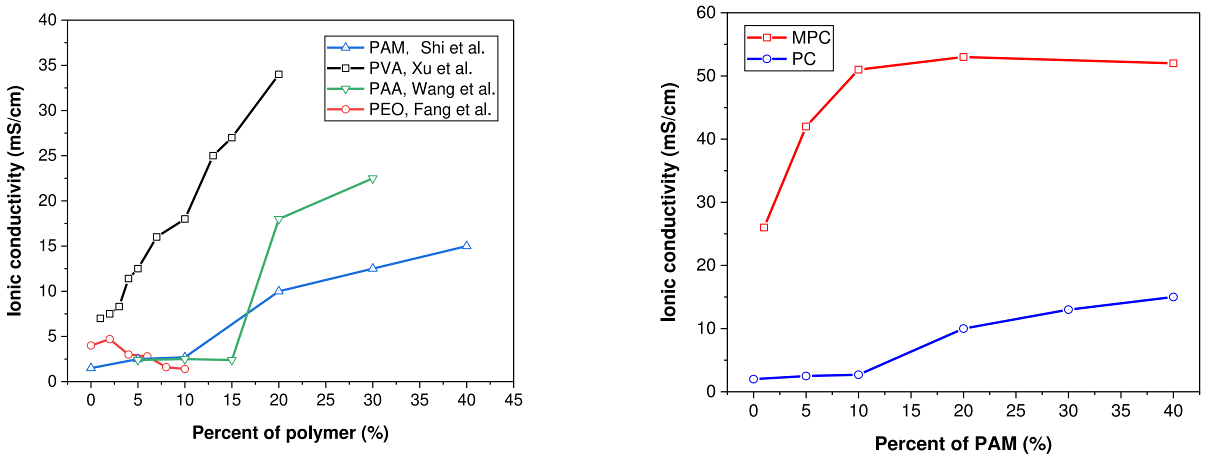

(e) Different polymer contents

(f) Different PAM content on PC- and MPC-based electrolytes

Fig. 16. (*continued*).

on ion transfer. Fig. 16 (f) shows the variation of their conductivity for MPC and PC with different PAM contents. Obviously, the electrical conductivity of MPC is much higher than that of PC due to the presence of magnesium oxide (MgO), potassium carbonate (KDP) and other substances in MPC, which have more conductive ions than OPC.

In addition, there is a direct relationship between the ionic conductivity and the porosity. Fig. 17. shows the effect of two polymers on these properties at different content levels. Initially, the ionic conductivity of the composite with PAA is low, about 0.2 mS/cm. As the increase in PAA content, the ionic conductivity increases significantly, sharply from 4 wt % of PAA, and reaches above 3 mS/cm at 8 wt% of PAA. The porosity of PAA samples was initially high, above 30 %, but decreases to about 10 % as PAA content increases. PAA is a polymer with a carboxyl (–COOH) functional group. The group can dissociate in an alkaline environment to form negatively charged carboxylate ions (COO^-), which increases the number of free ions in the system and thus improves the ionic conductivity. It also acts as a binder inside the cement paste. The long chain structure of PAA can fill the voids in the cement matrix and reduce the internal voids and pores. This makes the cement matrix structure denser, thereby reducing the overall porosity. The cement samples with 2 wt% of PEO exhibit the best ionic conductivity while the porosity increases steadily with increasing PEO content. A higher PEO content leads to an enhanced cross-linking or aggregation effect of the polymer chains, which limits the free movement of ions and results in a decrease in conductivity. Meanwhile, PEO is a highly hydrophilic polymer that strongly absorbs water. As the PEO content increases, more water is absorbed, causing it to expand. This expansion effect increases the pores and free volume in the cement matrix, causing the porosity to gradually

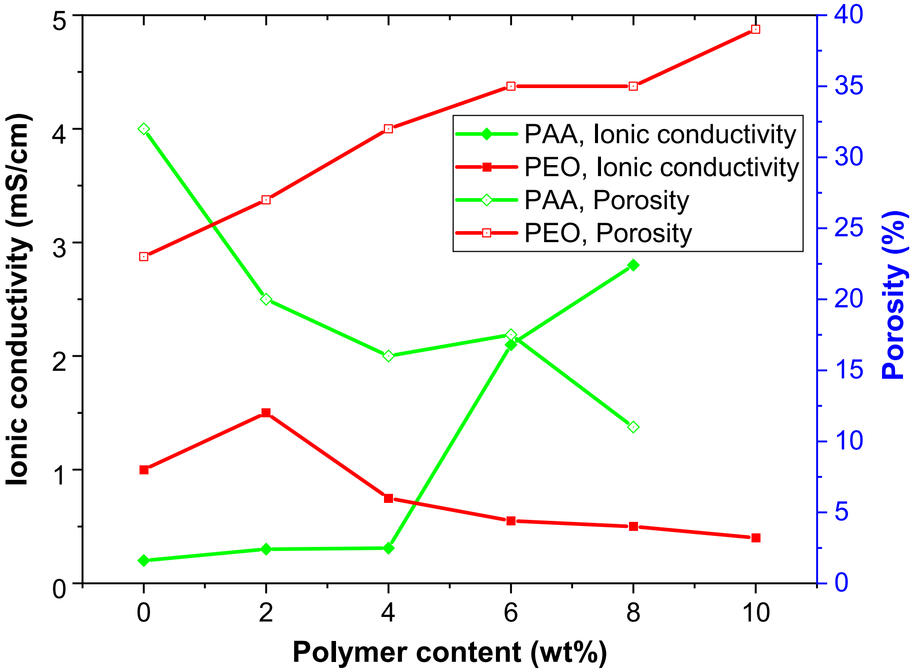

Fig. 17. Ionic conductivity and porosity comparison [57,100].

increase.

4.2.2. Effects of specific capacitance

Figs. 18 (a) to (d) show the electrochemical characterization of 3 types of cement. In the same system, the difference between the CV curves of MPC- and OPC-based electrolytes is significant shown in Fig. 18 (a), where the CV curve of OPC is almost a line and MPC is nearly a rectangular shape, meaning that the capacitive behaviour is much better in the MPC-based electrolyte. In Fig. 18 (b), the area of GCD curves of CA-based electrolyte is much larger than the other two electrolytes. But their shapes are all nearly triangle identifying a double layer capacitive behaviour. The situation of EIS curves of three electrolytes is consistent with the results of CV and GCD curves, as shown in Fig. 18 (c). The internal resistance from high to low is ordered OPC, MPC, and CA. Fig. 18 (d) shows the specific capacitance of three different types of cement. CBSC made with MPC and CA will have more conductive ions in the slurry state for PC vs. MPC electrolytes. In addition, the pores of the cement-based electrolyte in the former were saturated by soaking in the 1 mol/L KOH solution, while the latter were saturated by 2 mol/L solution. The increase in ion concentration will also affect the capacitance. However, it should be noted that an increase in ion concentration leads to a rise in internal resistance, meaning that higher ion concentration does not necessarily equate to better performance. It should also be noted that the specific capacitance of CA-electrolytes is significantly better than the first two. However, this is more related to the choice of electrode materials and will be discussed in the following sections.

Fig. 19 gives the effect of polymers on cement-based electrolytes. These structural supercapacitors possess typically electrochemical double-layer capacitance nature because all the CV curves appear to a spindle shape without any redox peak, as shown in Fig. 19 (a) to 19 (c). For PVA and PAA, their area of CV curves becomes larger as the polymer content increases, but the optimal content of PAM is not the highest content. 10 % of PAM causes the resistance to decrease to the lowest. After the dosage is more than 10 %, the interfacial contact is weakened, and the interfacial impedance increases significantly. The GCD curves show the same trend about polymer additives, as shown in Fig. 19 (d) and 19 (e). Fig. 19 (f) compares the effect of different levels of PVA, PAM and PAA on the specific capacitance of the cement-based electrolyte. The addition of PAM allows the MPC-based electrolyte to achieve a higher specific capacitance, which is maximized at 10 %. For PC-based electrolytes, PAA was clearly superior to PVA. This phenomenon is attributed to the good water solubility of PAA and the porous structure of the cement/polymer composite, which absorbs more conductive ions and ensures good wettability between the electrode and the electrolyte, as well as reducing the charge transfer resistance of the electrolyte and

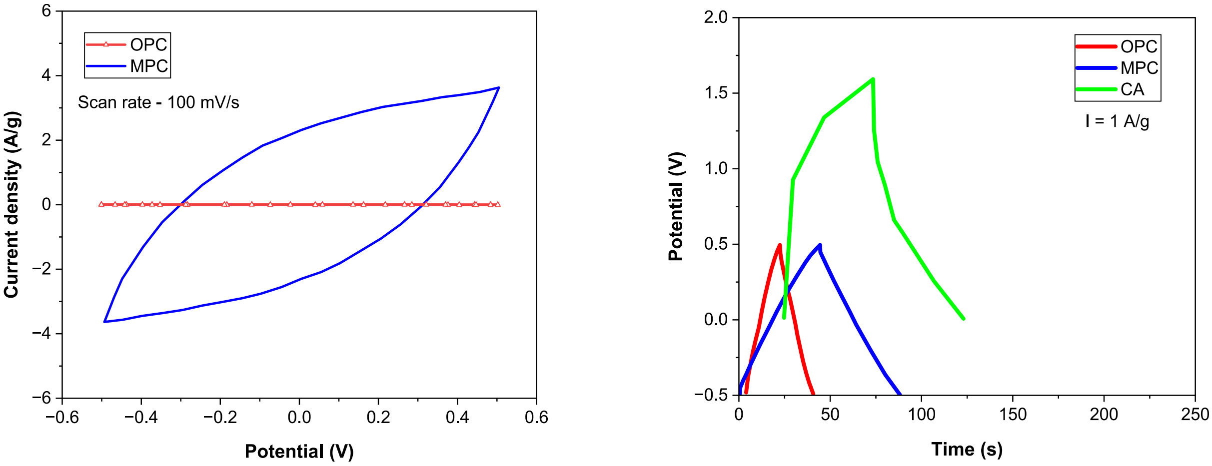

(a) CV curves

(b) GCD curves

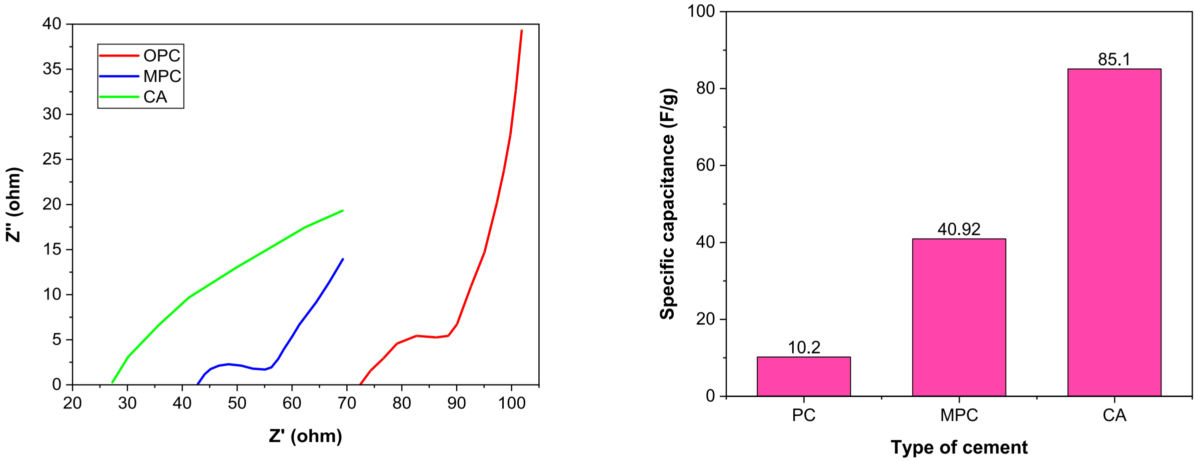

(c) EIS curves

(d) Specific capacitance

Fig. 18. Effect of the types of cement [10,85,86].

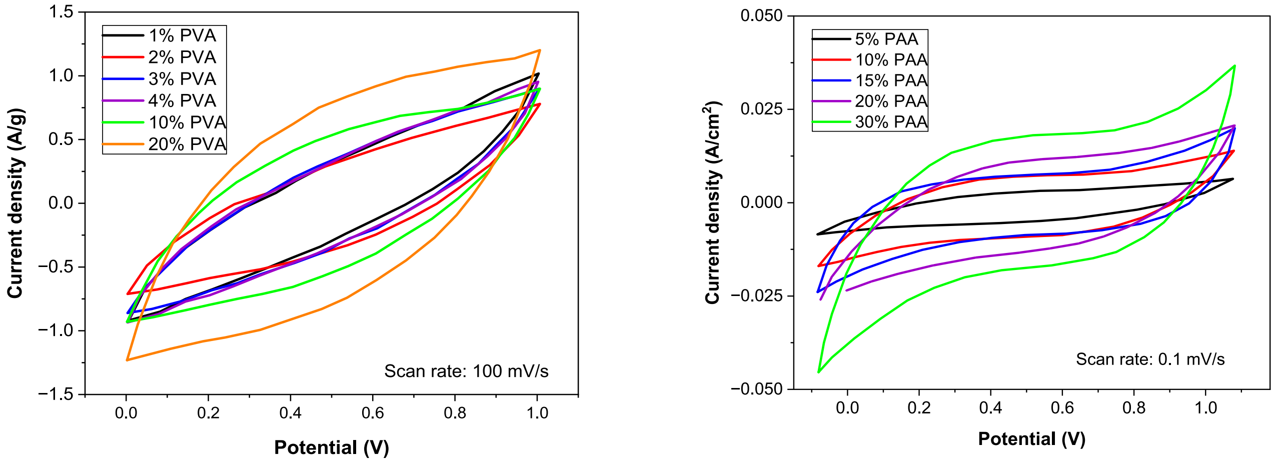

(a) CV curves of PVA/OPC

(b) CV curves of PAA/OPC

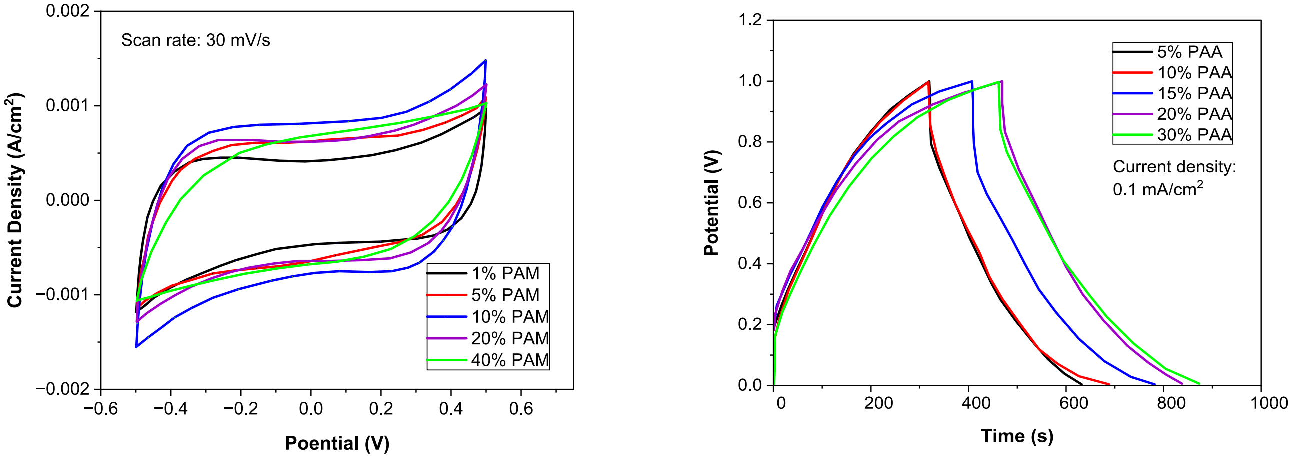

(c) CV curves of PAM/MPC

(d) GCD curves of PAA/OPC

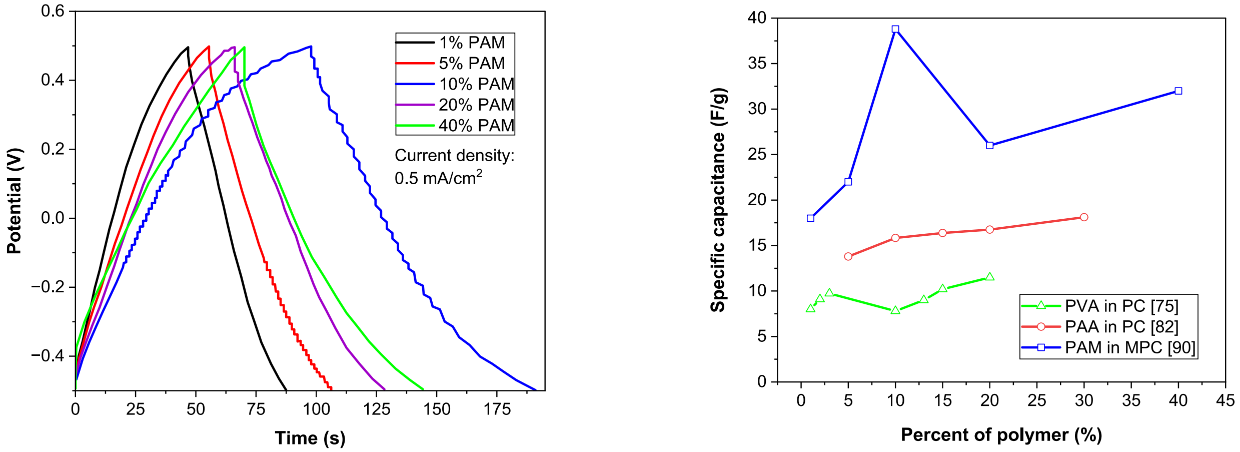

(e) GCD curves of PAM/OPC

(f) Trend of specific capacitance

Fig. 19. The effect of additives on polymer/cement-based electrolytes [59,96,104].

the electrode [122].

In addition, the solution in the pores of cement-based electrolytes has a significant impact on the capacity of CBSC. Zhan et al. [123] did not specifically introduce any pore solutions, meaning the solution present in the pores was limited to the water inherent in the material. Consequently, the obtained specific capacitance was significantly lower than that of CBSC using the same electrode but with the KOH-containing pore solution, highlighting the influence of potassium ions on electrochemical performance. On the one hand, the larger size of K^+ leads to weaker interactions with other molecules [124], accelerating ion transport in the electrolyte [125]. On the other hand, the ability of K^+ to improve high-rate capacity demonstrates the faster transport of non-aqueous K^+ electrolytes when compared to other ions [126–128]. Therefore, having an appropriate pore solution is one of the key points to optimize the electrochemical performance of CBSC.

4.2.3. *Effect of electrodes*

Charge storage and capacitance are highly influenced by the electrode material, which plays a crucial role in determining the electrochemical properties of a supercapacitor [15]. The active surface area of the electrode directly impacts capacitance, while pore size also affects the available surface area for ion adsorption and charge storage. Fig. 20 (a) shows the relationship between pore size and normalized capacitance, from which we can see that larger or smaller aperture size results in a significant decrease in capacitance [129]. Different types of electrode materials can also have a significant effect on the electrochemical properties of supercapacitors. Fig. 20 (b) compares the specific capacitance of supercapacitors using four electrode materials, including carbon, conductive polymers, metal oxides, and composites [130–133]. Carbon-based materials, such as graphene, CNTs and nanocarbon black, are often used as electrodes in CBSC due to their high electrical conductivity, high specific surface area, tunable porosity, excellent electrochemical stability, and long-life cycle [134–136]. In addition, the effect of the difference in specific surface area on the capacitance should not be neglected, as shown in Fig. 20 (c).

4.2.3.1. Areal capacitance. Most of the electrodes selected in the study of CBSC are composite electrodes, which usually consist of carbon nanomaterials, metallic materials, and metal oxide materials. Carbon-based materials can provide high surface area and excellent electrical conductivity, and metallic materials are able to undergo redox reactions, thus providing a large amount of pseudocapacitance. The combination of the two materials and exploration of the properties of the different materials to design electrode materials with high capacitance are

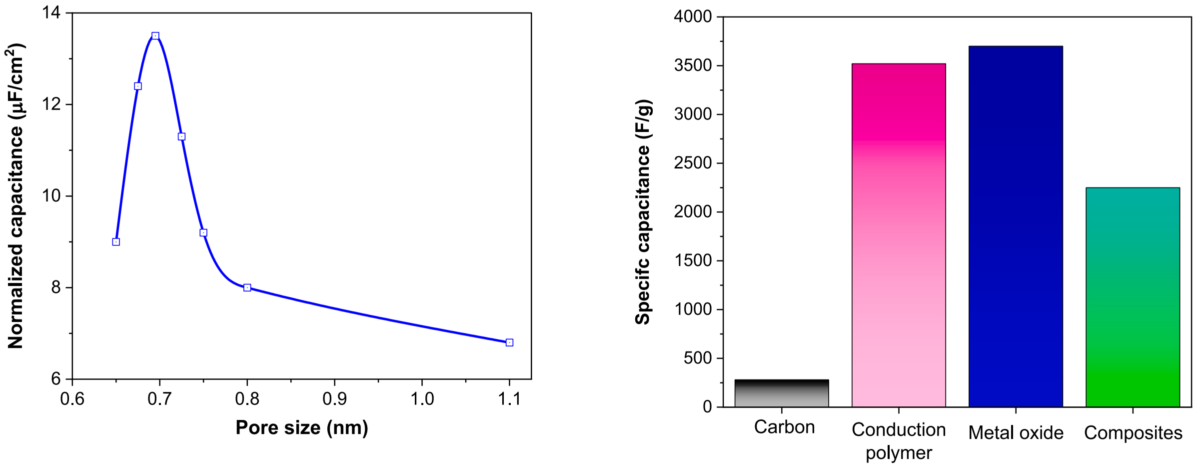

(a) Pore size and normalized capacitance

(b) Specific capacitance of different electrodes

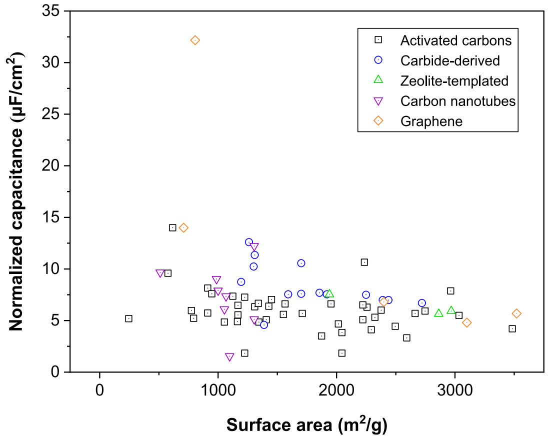

(c) Different specific surface areas of carbon materials

and normalized capacitance

Fig. 20. Relationship between electrode materials and electrochemical performance of supercapacitors [43,129,131,137–145].

primary goals in the field of supercapacitors.

Fig. 21 shows the SEM of the microstructure of composite electrodes. The rGO electrodes show the uniform 3D nanosheets in Fig. 21 (a), while the well-distributed 3D petal nanoflakes are presented in Fig. 21 (c), where rGO is coated on the surface of Ni foam evenly and completely. Their microstructure is similar because they are not deeply integrated, but the rGO is simply coated on metal foam. The microstructures of rGO/monometallic oxide are presented in Fig. 21 (b), 21 (d), 21 (g) and 21 (h). Fig. 21 (b) shows gelatinous rGO/MnO_2 where MnO_2 nanosheets are encapsulated in rGO and Fig. 21 (d) shows many CuO microspheres are attached to the rGO surface with ordered distribution, which is good for conductivity. This is also proved by electrochemical measurements. Flower clusters of SnO_2 grow and emerge forming a multi-layer porous structure with macropores, which is beneficial to ion transport, as shown in Fig. 21 (g). The Fe_2O_3 is attached and dispersed evenly on the rGO nanosheets and the rGO/Fe_2O_3 has cubic characteristics. Compared to rGO/monometallic oxide electrodes, the rGO/complex metal oxides electrodes are more complicated, such as rGO/$NiCo_2O_4$ and rGO/$CuCo_2O_4$. In Fig. 21 (e), the $NiCo_2O_4$ nanosheets cover the rGO nanoflakes and are well-distributed on the rGO, while the clusters of aggregates began to form due to the cross of $NiCo_2O_4$. In Fig. 21 (f), $CuCo_2O_4$ particles are encapsulated in the rGO nanoflakes, forming flower-like microspheres. These two rGO/complex metal oxides both generated spherical aggregate, which means the composition of the electrode is more complex offering higher surface area. The last one is rGO/Ni_1Co_1S electrode and uniform large sheets interconnecting with each other as shown in Fig. 21 (i). A 3D nano hydrangea-like structure grows on the surface of rGO, which can provide larger surface area, redox reaction active sites and porous channels for ion diffusion in the electrodes.

Figs. 22 (a) and 22 (b) give the CV curves of seven electrodes at 50 mV/s and 5 electrodes at 10 mV/s. The black curve in Fig. 22 (a) is the CV curve of rGO, which shows the EDLC performance with a nearly rectangular shape. The CV curve of rGO/Ni foam and rGO/Fe_2O_3 is almost same as rGO, except the area of CV curve rGO/Ni foam and rGO/Fe_2O_3 is bigger, which means that these electrodes can absorb or release more energy. Interestingly, the CV curve of MnO_2 is contained in rGO, but the CV curve range of rGO/MnO_2 exceeds the rGO and has a shaper peak. This explains that the combination of carbon and metal oxide materials can exploit their electrochemical advantages to achieve the cooperation between the EDL effect and the pseudocapacitive effect. There are more metal elements in the rGO/$CuCo_2O_4$ and rGO/Ni_1Co_1S electrodes, which makes the CV curves more irregular. The condition represents that the pseudocapacitive effect dominates the capacitive effect inside the electrodes, as well as the occurrence of a more abundant and complex redox reaction. In addition, the CV curve of rGO/CuO electrode is listed separately because its area is larger than others and cannot be drawn at the given coordinate interval. In Fig. 22 (b), the area of CV curves of rGO/$NiCo_2O_4$ and rGO/SnO_2 electrodes is larger than others. However, the shape of the rGO/$NiCo_2O_4$ is quasi-rectangular, characterizing the electrode belonging to EDLC because the pseudocapacitive properties of $NiCo_2O_4$ are covered by rGO. The rGO/SnO_2 shows the obvious pseudocapacitive properties with a very irregular curve. Moreover, a high scan rate always leads to a limitation of ion diffusion, resulting in the reduction of peak current, and the Y-peak value can prove it. The peak current value and shape on the CV curves of Ni foam, Fe_2O_3 and Ni_1Co_1S at 50 mV/s are lower and smaller than the curves at 10 mV/s. The reason is that mass transport limitation occurs when the electrochemical reaction rate exceeds the mass transport rate at a higher scan rate.

Fig. 22 (c) shows the GCD curves of eight electrodes at 1 mA/cm^2 of current density. The GCD curves of seven electrodes are almost equilateral triangle shapes except for the rGO/Ni_1Co_1S electrode. This

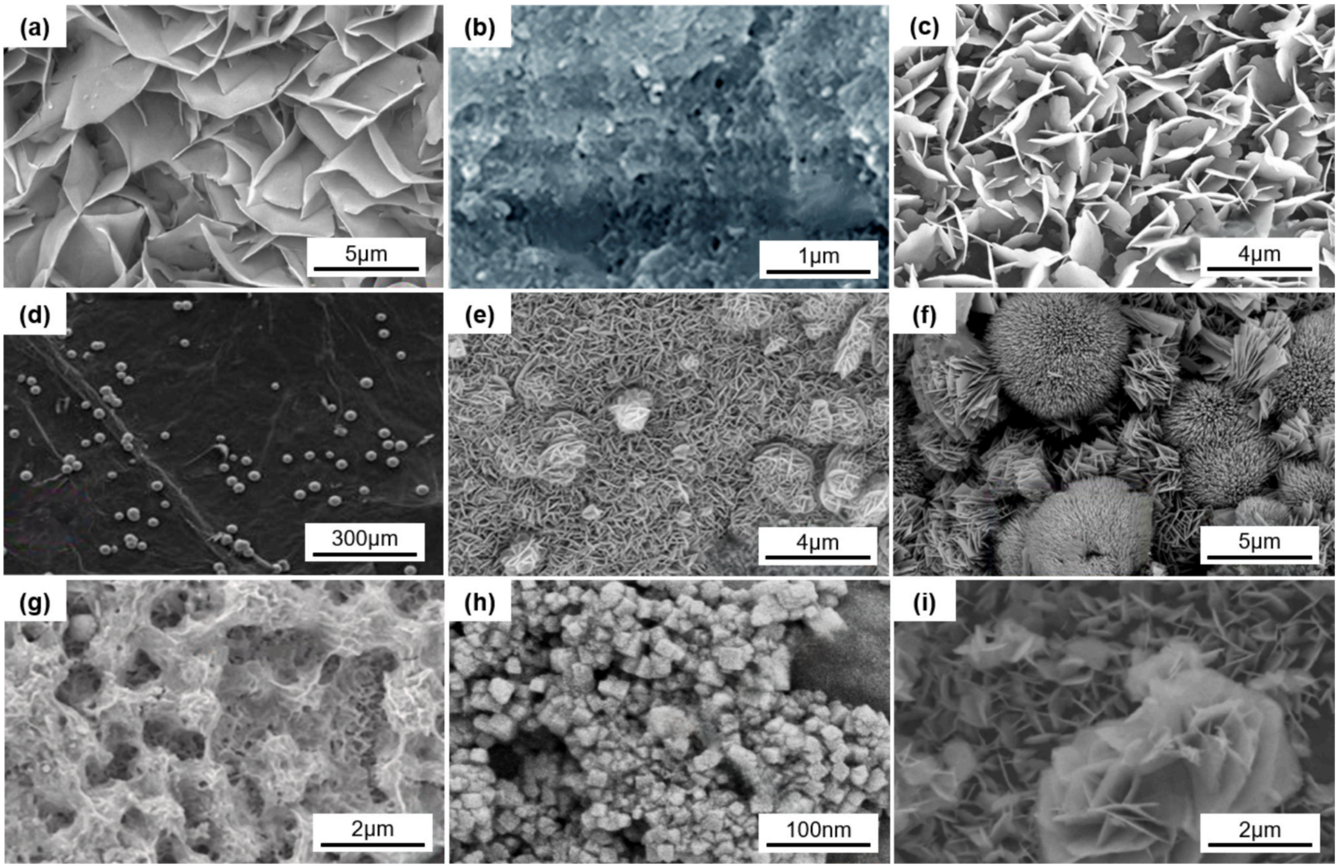

Fig. 21. The SEM of electrodes (a) rGO, (b) rGO/MnO_2, (c) rGO/Ni foam, (d) rGO/CuO, (e) rGO/$NiCo_2O_4$, (f) rGO/$CuCo_2O_4$, (g) rGO/SnO_2, (h) rGO/Fe_2O_3, (i) rGO/Ni_1Co_1S [18,57,58,61,100,101,146–148].

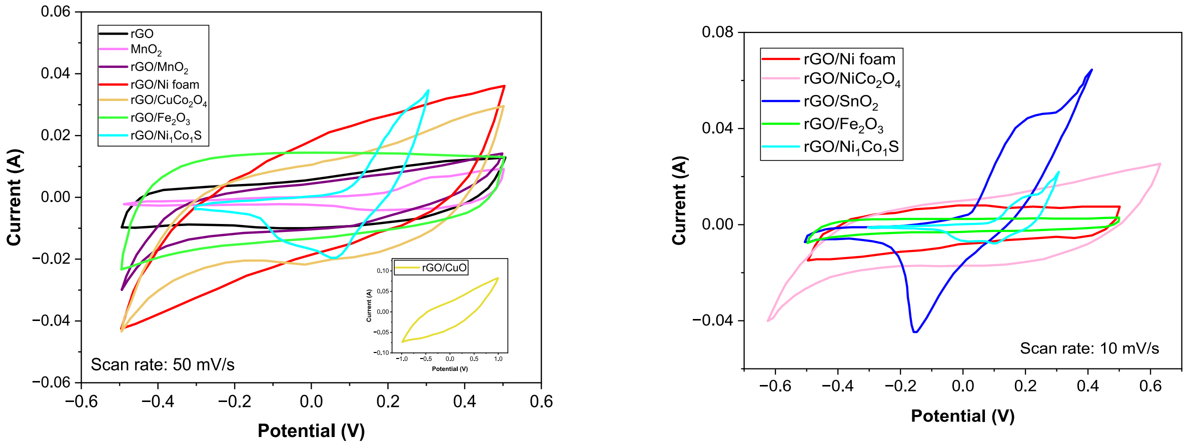

(a) CV curves of at 50mV/s

(b) CV curves at 10mV/s

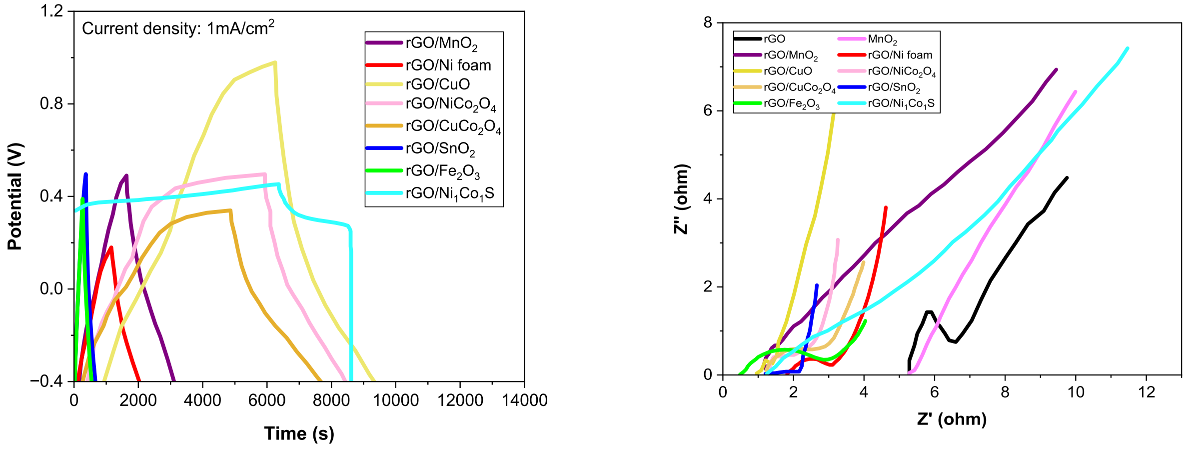

(c) GCD curves at 1 mA/cm^2

(d) EIS curves

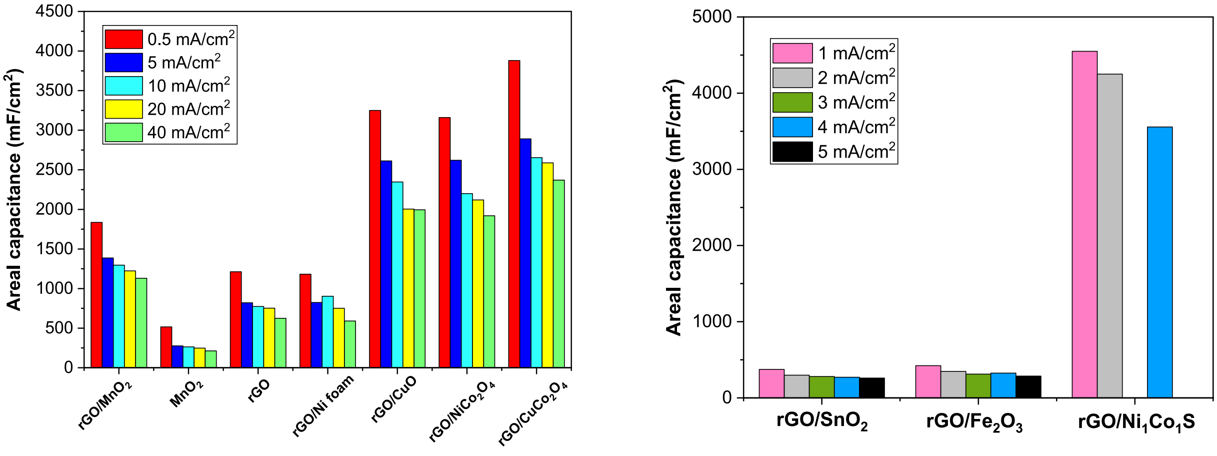

(e) Areal capacitance at 0.5-40 mA/cm^2

(f) Areal capacitance at 1-5 mA/cm^2

Fig. 22. Comparison of electrochemical characterization of different electrodes [18,57,58,61,100,101,146–148].

represents their electrochemical capacitive behavior is apt to EDLC nature and the charge–discharge process is efficient, which is nearly consistent with CV results. It should be noted that the pseudocapacitive behavior of some electrodes is not presented by the GCD curves but presented by CV curves due to their pseudocapacitance nature hidden by EDLC nature of rGO probably. The rGO/CuO and rGO/Ni_1Co_1S cover the largest GCD area, suggesting good electrochemical behavior, coulombic efficiency and conductivity[61].

Fig. 22 (d) is the EIS curves as well as the Nyquist plots, which represent the internal resistance of electrodes. The internal resistance of the individual rGO or MnO_2 electrode is bigger than the composite electrodes, but it will decrease a lot after the combination of carbon and metal materials. The rGO/CuO and rGO/Ni_1Co_1S have the lower resistance which adhere to their CV and GCD results. However, the electrode with the lowest internal resistance is the rGO/Fe_2O_3, but its CV and GCD results are not the best, which shows that the electrochemical reaction is not strong. Therefore, the selection of materials needs to be considered in many aspects.

Fig. 22 (e) and Fig. 22 (f) give the areal capacitance of the electrode material at different current densities. The areal capacitance decreases as the current density increases. In other words, these electrodes have ideal capacitive behavior in the low-frequency range, which is consistent with the theory of EIS [149]. In the design of electrode materials for CBSC, carbon nanomaterials are generally combined with metal oxides to form composite electrodes, preferably in an asymmetric form. This is because this form of electrode can provide a broader range of operating voltages, thus further increasing energy density [17,150–152]. Composites can combine the properties of different materials to meet the need for high energy density and high-power density [153,154]. Carbon materials can provide physical support and charging transport channels. Especially the carbon nanostructures has high electrical conductivity, which helps to realize the high-rate capacity of CBSC [155], while the metal oxides are the main site for energy storage [156,157]. For example, electrodes made of rGO with Cu have very high areal capacitance due to the presence of more active sites on the surface of the composite electrode [158]. However, almost no conductive polymers have been used to make electrodes for CBSC, so this could be one of the future research directions. To further understand the reaction mechanism of these electrodes during charging and discharging, Table 5 concludes their equations of reduction or oxidation.

4.2.3.2. Capacitance retention. Capacitance retention of electrodes has a significant impact on the use of supercapacitors. It is the retention of the electrical capacity of a device relative to its initial value after a given number of charge/discharge cycles [159]. Fig. 23 shows the capacitance retention of selected CBSC electrodes (anodes) at different current densities or voltage change rates. The capacitance retention of the composite electrodes is greater than 80 %. The capacitance retention of rGO/$NiCo_2O_4$ nanosheets and rGO/$CuCo_2O_4$ nanowires remains above 85 % after 10,000 charge/discharge cycles, which suggests that nanomaterials can have a significant impact on improving retention [160,161]. On the contrary, compared to the rGO/NCM-S electrode, which also used Ni and Co elements, its capacitance retention decreased to 80 % after only 5000 cycles, illustrating the above point. In addition, the combination of carbon-based materials and metal oxides leads to the interplay of faradic and non-faradic charge storage mechanisms, allowing for higher cycling stability [138,162].

5. Multifunctionality and applications of CBSC

5.1. Multifunctionality

CBSC is a multifunctional structure, so they have the electrochemical functions, such as storing and releasing large amounts of charge, but also need to be able to withstand mechanical loads, thus realizing multiple, predetermined functions to meet specific requirements [163]. However, an obvious conflict exists between the mechanical properties and the electrical demands of structured supercapacitors, as shown in Fig. 24 (a). Fig. 24 (b) shows the relationship between normalized capacitance and normalized hardness (water-to-cement ratio) [39]. This illustrates that while high-rate capacity can be achieved with high W/C cement electrode materials, material strength is sacrificed. In all relevant studies to date, there is a significant conflicting relationship between these functionalities [20]. This makes the design of solid electrolytes not a simple mixing of materials, but rather a tradeoff balance the relationship between their electrochemical and mechanical properties, such as increasing the specific capacitance and compressive strength of the material while increasing its ionic conductivity.

Based on the existing studies related to CBSC, their compressive strength was plotted against specific capacitance for different parameters, as shown in Fig. 24 (a). Its development pattern shows a paradoxical relationship between mechanical and electrochemical properties. As the specific capacitance increases, the mechanical strength decreases. However, as in the region within the pink circle in the figure, this region represents the optimal multifunctionality of the material, or the paradoxical relationship is beneficially mitigated. Therefore, the multifunctionality is being moved to the pink area in the upper right corner of the figure to strengthen the multifunctionality of the energy storage structure for commercial applications. Based on this purpose, we consider two perspectives for the study. One is to study the capacitive behavior of high-performance cement/concrete from its piezoresistive and conductive properties. Current research on self-sensing cement/concrete is very intensive, and this type of material can be made into various types of sensors for dynamic monitoring of structures [167–174]. The principle is due to the transfer of electrons generated internally, and the principle of the path that realizes the energy storage cement is similar [175]. As a result, optimization of self-sensing cement/concrete is one of the most convenient, simple, and reasonable directions.

On the other hand, we can choose to start with a solid supercapacitor with good performance and adjust the electrolyte composition to meet civil engineering requirements [176]. A considerable number of solid-state supercapacitors have been fabricated, which also have very good performance [177], while CBSC have received a lot of attention in recent years and have been used to achieve energy storage properties by adding carbon nanomaterials, conductive polymers, and metal compounds to cement [39,101,165,178]. However, this is contrary to the conventional understanding, and the solution to this problem can be derived from alleviating the conflicts between strength and toughness of materials [179]. Some materials, like human cortical bone, increase external

Table 5
The redox reactions and merits of the anode materials.

Anode materials	Reactions	Merits	Refs.
rGO/MnO_2	$MnO_2 + 2H_2O + 2e^- \leftrightarrow MnO(OH) + OH^-$	Improve electrochemical performance	[57]
rGO/Ni foam	$Ni(OH)_2 + OH^- \leftrightarrow NiOOH + H_2O$	Ni and rGO can both increase the specific surface area	[146]
rGO/CuO	$CuO + 2e^- \leftrightarrow Cu + O^{2-}$	Increase areal capacitance and power density	[101]
rGO/$NiCo_2O_4$	$NiCo_2O_4 + 2OH^- \leftrightarrow NiOOH + CoOOH + H_2O + 2e^-$	Increase current density	[147]
rGO/$CuCo_2O_4$	$CuCo_2O_4 + 2OH^- \leftrightarrow Cu(OH)_2 + Co(OH)_2 + H_2O + 2e^-$	utilize the excellent capacitance of metal oxides	[100]
rGO/SnO_2	$SnO_2 + 4e^- \leftrightarrow Sn + 2O^{2-}$	Provide excellent rate capability	[58]
rGO/Fe_2O_3	$Fe_2O_3 + 6e^- \leftrightarrow 2Fe + 3O^{2-}$	Low internal resistanceEnsure favorable charge transfer and fast ion diffusion	[18]

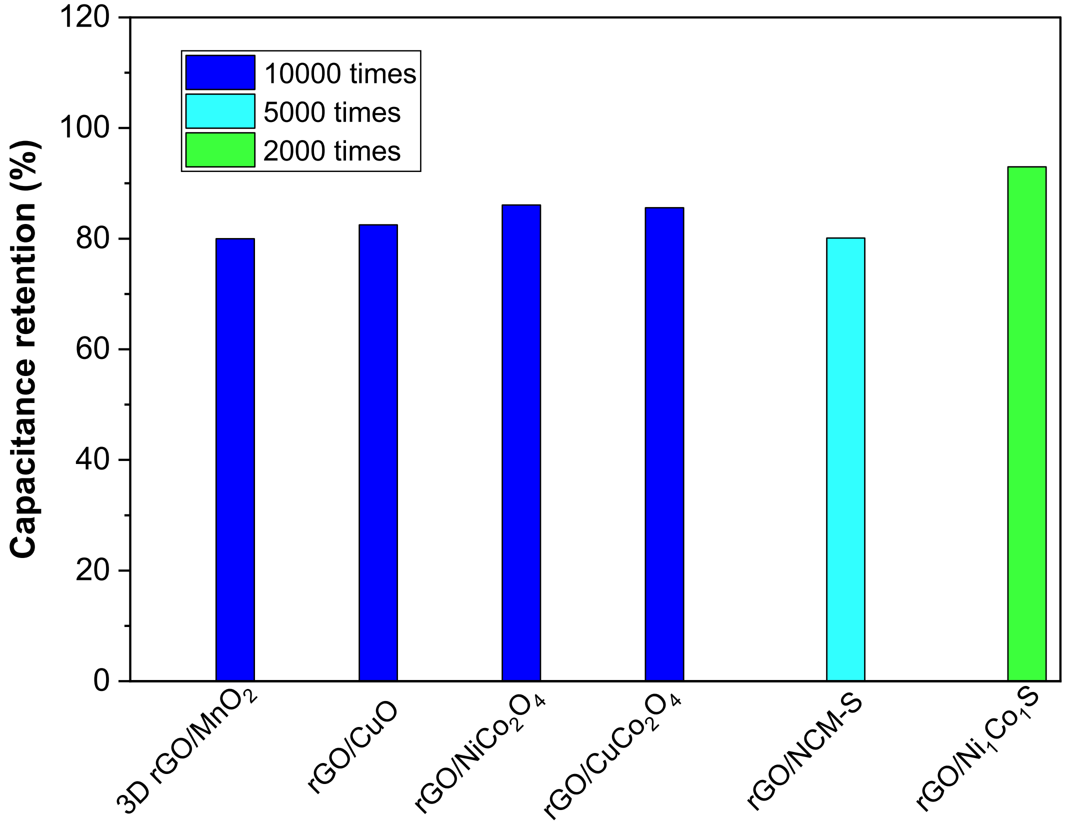

Fig. 23. Capacitance retention rate of different electrode materials at the current density of 10 mA/cm^2 [57,58,61,97,100,101,147,148].

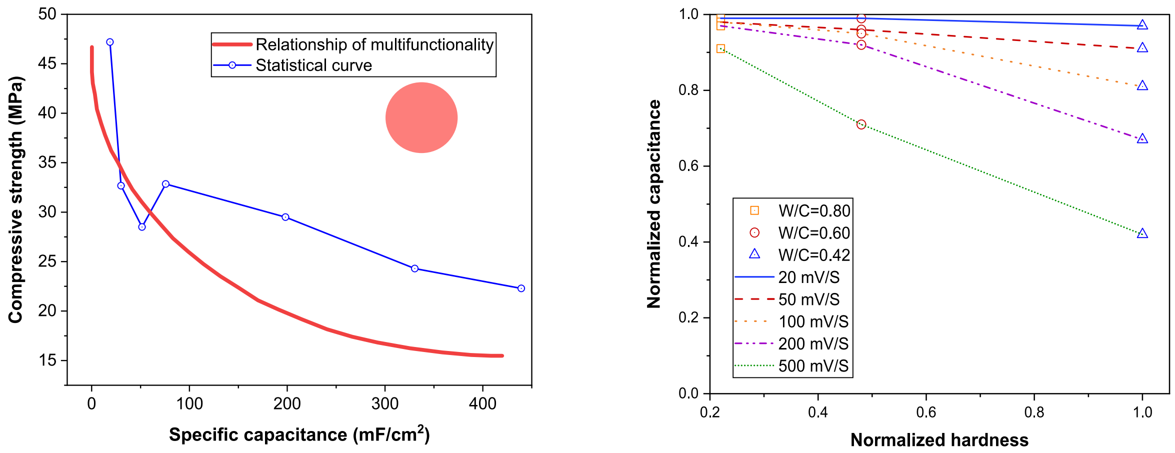

(a) Comparison of compressive strength with specific capacitance

(b) Relationship between normalized capacitance and hardness

Fig. 24. Relationship between properties of Cement-based supercapacitors [39,164–166].

strength and internal toughness through intrinsic and extrinsic toughening. Similarly, craftsmanship is used to strengthen the skeleton of the energy storage structure to achieve the desired mechanical strength and improve the electrochemical properties of the rest of the structure to ensure that the overall structure is electrically conductive. In addition, the formation of conductive networks and ion transport channels is random due to the irregular distribution of conductive additives within the cement. Therefore, the addition of self-healing polymers capable of spontaneous polymerization [180,181] or cross-linking reaction [182,183], is considered to form channels for charge and electron transport [184,185].

5.2. Applications

In recent years, the development of energy storage building materials has gained significant attention from both scientists and governments worldwide. This is largely due to the substantial greenhouse gas emissions from the construction sector, which contribute 8 % of global emissions. As a result, creating energy storage solutions for sustainable infrastructure is a critical and necessary step for the cement industry. One potential solution for the energy transition is transforming building structures into energy storage systems, helping to reduce the industry's environmental footprint.

Fig. 25 (a) shows that the energy is stored on the surface of the brick supercapacitor with capacitive nanofibrillar PEDOT coating, which can light up a green light [186]. Three supercapacitors connected in series can withstand a 3.6 V window and the CV curve of the device is exhibited in Fig. 25 (b). The application of CBSC is closely related to renewable and electrical energy, intending to quickly store peak power for later retrieval. According to Massachusetts Institute of Technology (MIT), a 45-cubic-meter block of nanocarbon black cement can store about 10 kWh of energy after a one-day charge from solar panels, equivalent to the average daily electricity use of a household [39]. At the same time, supercapacitors of this size can be integrated into the foundations of buildings, and more importantly, this does not increase construction costs or reduce structural strength. A charged carbon-cement supercapacitor powers multiple LED lights and is connected to a multimeter to measure its voltage of the system at 12 V, as shown in Fig. 25 (c). If the same approach were applied to build roads, parking lots, or driveways, electrified concrete could store renewable energy, enabling electric cars to be powered via inductive chargers. Fig. 25 (d) gives the CV curves of CBSC with different carbon types at 50 and 100 mV/s of scan rate. This illustrates that the carbon nanomaterials could enhance the capacity of cement to store energy because the carbon black is self-assembling into a connected conductive wire, but the level may be influenced by the pore surface distribution of the materials. A rechargeable cement-based battery with an average energy density of 7Wh/m^2 has been also developed successfully, as shown in Fig. 25 (e) [187]. Short carbon fibers (CF) were added to the cement-based electrolytes to improve the conductivity. The anode and cathode are iron-zinc and nickel-based oxides respectively. The device can make a little LED light bright for a few hours.

In the future, the commercialization and large-scale deployment of this energy storage technology will have a transformative impact on the global energy landscape. For instance, the construction of large hydroelectric power plants requires millions of cubic meters of cement, which currently serves only as structural support. If electricity generated by these plants could be stored directly within the concrete structures, it would substantially lower the construction costs associated with traditional storage facilities. The widespread use of energy storage cement in power plants worldwide could not only reduce costs but also significantly lower greenhouse gas emissions, contributing to the gradual achievement of carbon neutrality.

Overall, not only CBSC, but almost all solid supercapacitors face 3 challenges. For cement-based electrolytes, look for an additive or additives that will allow the electrolyte to produce energy storage capacity while bonding well with the materials in the cement during the hydration process and providing sufficient mechanical strength. In addition, the development of low-carbon cement-based supercapacitors not only has the function of storing energy and carrying loads but also can further reduce greenhouse gas emissions. For electrode materials, although some already have relatively good electrochemical properties, most are consumable and not sustainable. If improperly handled, it can cause irreversible and harmful effects on the environment, such as heavy metal contamination [188]. Therefore, the development of green electrode materials is of great importance. Finally, interfacial problems are also difficult to solve. The most important issue is the contact problem between the electrolyte and the solid particles on the electrode's contact surface. If the contact is incomplete, even if the electrode or electrolyte has good electrochemical properties, it will not be fully effective. Overcoming interfacial problems by increasing the contact area, introducing buffer layers, or using wetting agents [11] is a very promising direction. In addition, there is scarce literature on the development of electrochemical properties of CBSC under load. Therefore, more studies are needed to support the effect of CBSC's performance under various variable conditions.

6. Challenges and discussions

Cement-based supercapacitors face three main challenges: optimization of cement-based electrolyte materials, optimization of electrode materials, and improvement of the electrolyte/electrode interface. First, unlike other solid supercapacitor electrolytes, such as gel polymers, cement does not have inherent conductivity and energy storage properties [189–191]. Cement electrolytes can only be made to meet the requirements by adding various conductive materials (polymers, carbon nanomaterials) to the cement and forming conductive networks and pores inside that can adsorb charges [101,192,193]. Therefore, the choice of additives is critical to the development of energy storage capacity. In addition, the low toughness of cement limits the change in ion volume during charging and discharging, which leads to the degradation of energy storage performance [11,17,194]. Therefore, for cement-based electrolytes, good electrochemical properties are ensured while considering their strength and toughness. Another major drawback is that ion diffusion in this electrolyte depends on the contact of solid particles [195,196]. Especially for points of mutual contact with the electrode material, they are particularly sensitive to stresses that develop during electrochemical cycling in electrode materials [197]. These stresses can cause cracks to form and propagate [198], as well as lead to interface delamination [199,200].

The selection of electrode materials should be paid more attention. It has been proved that nanomaterials can provide many active sites for electrochemical reactions due to their extremely high specific surface area. This advantage leads to an increase in capacitance and improves the electrical and electrochemical performance index significantly [201–203], as shown in Table 6 Nanomaterials are the foremost selection for electrode materials, which contributes to the advancement of supercapacitor technology.

In CBSC, composites of metal oxides and carbon nanomaterials have become mainstream as electrode active materials that can improve electrochemical performance and cycle stability [209,210]. Therefore, making full use of the advantages of different materials and combining them through reasonable matching is one of the focuses of electrode material development in the future [211–214].

Moreover, developing green and sustainable electrodes minimizes environmental pollution [201]. Carbon materials of various plant origins, including activated carbon from agricultural waste [215], biomass-derived carbon [216], seaweed-based carbon [217], silk-derived carbon [218], cellulose-derived carbon [219] and lignin [220] and biodegradable polymers [221] are materials that can be used to make green electrodes. These materials are attracting increasing attention as "green electrodes" due to the demand for environmentally friendly energy storage technologies [222].

Finally, the interface problem between the electrode and the electrolyte severely limits the performance of CBSC [223]. It is widely known that the interface between the cement-based electrolyte and the electrodes is relatively poor, which usually leads to high internal resistance and hinders ion transport in supercapacitors. Therefore, CBSC should be carefully designed to achieve complete contact between them [224]. The source of ion transport resistance in solid electrolytes is the lack of physical contact between the solid particles [225,226]. In polycrystalline materials and composite electrodes, contact between solid particles must be maximized and maintained for effective ion conduction [227,228]. In contrast, the presence of pores implies tortuous ion conduction paths and inhomogeneous current densities. These effects contribute to the observed macroscopic ion transport resistance [151]. Therefore, effective densification of polycrystalline solid electrolytes and composite electrodes is essential for improved ion transport [229]. However, this can be a contradiction and a major challenge when considering the mechanical properties and processability [230–232] of

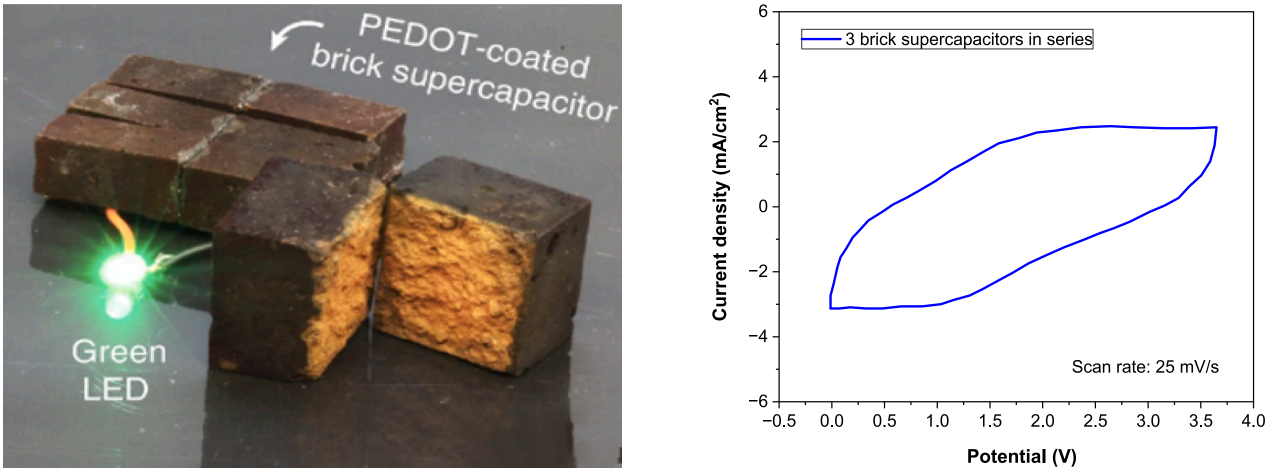

(a) Energy storage brick supercapacitors

(b) CV curve of the brick supercapacitors

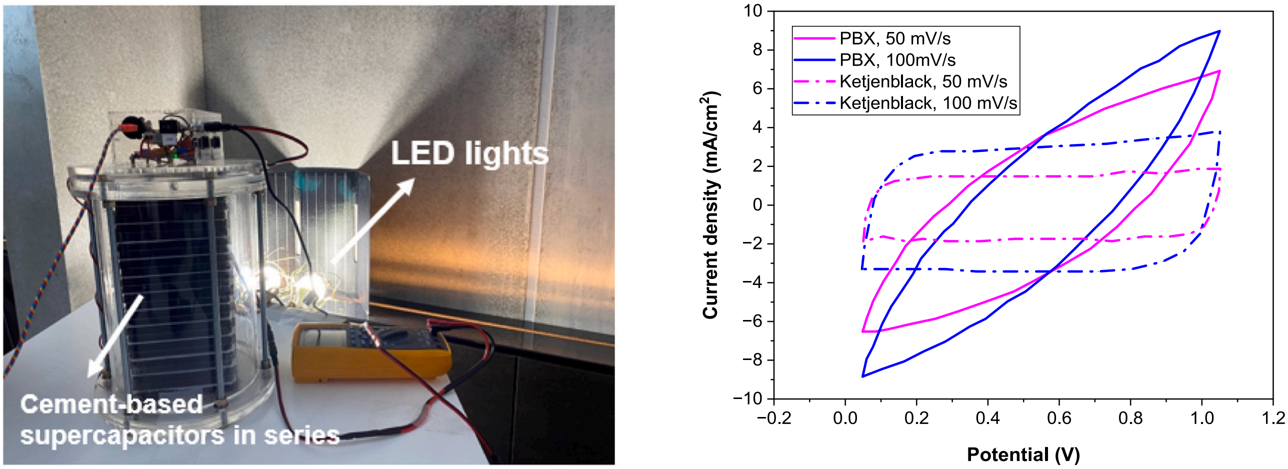

(c) Example of CBSC

(d) CV curves of CBSC

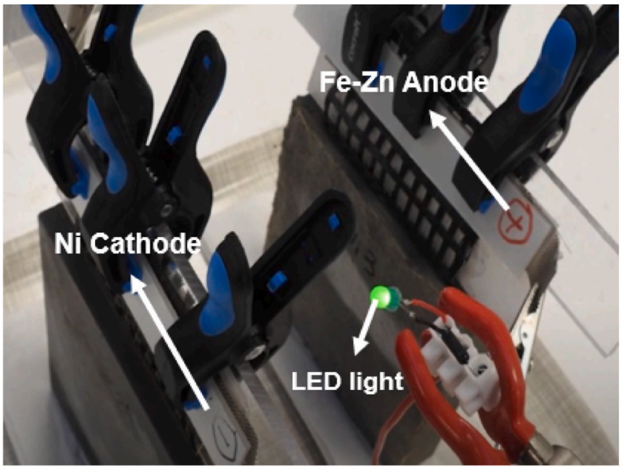

(e) Example of cement-based battery

Fig. 25. Schematic diagram of construction materials for energy storage application [39,185,186].

Table 6
Comparison of different nanomaterial electrodes.

Types	Characteristics	Functionalities	Examples	Refs.
Metal nanomaterials	Low internal resistance, good conductivity	High capacitance, long cycle stability	Gold, silver, copper, nickel	[203,204]
Metal oxides (MO)	High surface area, high capacitance	High energy density, high capacitance	Fe_2O_3, TiO_2	[203,204]
Carbon nanomaterials	High specific surface area, good electrical conductivity, low cost, good strength	High power density, long cycle life	Reduced graphene oxide, CNTs	[205–208]
Conductive polymer	Easy to synthesize, good conductivity	High capacitance, low cost	PAA, PAM, PEO	[206]

solid electrolytes and electrode materials [17,223].

7. Conclusions and perspectives

With the goal of global carbon neutrality and the urgent need to transition from fossils to renewable energy sources, energy storage cement/concrete has emerged as a novel and promising field. This paper reviews and discusses the development, design, and characterization techniques of cement-based supercapacitors in recent years. To develop cement-based supercapacitors with excellent mechanical and electrochemical properties, the key factors including cement types, W/C ratio, additives, electrodes materials, etc., have systematically been compared and analyzed. The main conclusions and observations are as follows:

(1) The energy storage mechanism of cement-based supercapacitors is a combination of the double electrical layer effect, redox reaction, and electrolyte energy storage mechanism. These mechanisms will work cooperatively to improve electrochemical properties, and the selection of materials plays an important role in their interactions.
(2) The mechanical strength of cement-based supercapacitors is affected by the type of cement, W/C ratio, curing time, and additives. The optimum W/C ratio should be around 0.42, which can mitigate the conflict between two properties. Special cement generally has higher compressive strengths than OPC, regardless of the setting time. In addition, the additives should interact with the molecules in the cement, e.g. through cross-linking reactions, to have a positive effect on compressive strength. In addition, a water-cement ratio too high or too low can adversely affect the electrochemical properties of cement-based electrolytes.
(3) The cement-based electrolytes, conductivity and specific capacitance are affected by cement type, polymer types and polymer content. Because MPC contains more ions, it has a higher conductivity and specific capacity than OPC, even with the same amount of polymer added. As the polymer content increases, the electrical conductivity of the cement matrix increases, and the specific capacitance essentially follows this pattern. However, the content of polymer should preferably not exceed 20 % according to the analysis. A higher percentage may cause a significant decrease in mechanical performance, but a slight increase in energy storage capacity although it will improve the ionic conductivity progressively.
(4) Nanocomposites of carbon nanomaterials and metal oxides are typically chosen as electrode materials for cement-based supercapacitors. The combination of these two nanomaterials can take full advantage of the high specific surface area, good electrical conductivity of carbon-based materials, low resistance, and excellent cycling stability of metal oxides. As a result, both the areal capacitance and the capacitance retention rate are improved.
(5) There is a clear tradeoff between mechanical and electrochemical properties in improving the multifunctionality of cement-based supercapacitors. This tradeoff may seem irreconcilable, but we may be able to solve this dilemma by creating an effective ion conduction network within the cement.
(6) More studies and layouts of structural supercapacitors, such as bridges, tunnels, high-rise buildings, etc., should be carried out to discover suitable structures to explore the characteristics of this new energy storage structure for practical applications. Consequently, cement/concrete structures for energy storage could be further investigated.

In conclusion, CBSC and most solid supercapacitors face three key challenges. First, optimizing cement-based electrolytes requires identifying additives that enhance energy storage capacity while ensuring strong bonding with cement during hydration and maintaining sufficient mechanical strength. Additionally, the development of low-carbon CBSCs, which combine energy storage with structural load-bearing capabilities, presents an opportunity to reduce greenhouse gas emissions. Second, while some electrode materials exhibit promising electrochemical properties, many are non-sustainable and consumable. Improper disposal can lead to severe environmental consequences, such as heavy metal contamination [188]. Therefore, the development of green electrode materials is of great importance. Finally, interfacial challenges remain a significant obstacle. The most critical issue is achieving effective contact between the electrolyte and solid electrode particles. Even if both components possess excellent electrochemical properties, poor contact renders them ineffective. Addressing this issue through strategies such as increasing the contact area, introducing buffer layers, or using wetting agents is a promising direction for future research [11]. Moreover, limited studies have explored the electrochemical performance of CBSC under load conditions. Further research is needed to assess their behavior under varying operational conditions and support their real-world application.

The sustainability enhancement of advanced CBSC not only reduces the environmental impact of the production process but also contributes to the application and development of green energy technologies. By utilizing common materials such as cement, these supercapacitors can provide cost-effective and sustainable energy storage solutions, thereby promoting economic growth and the efficient utilization of energy resources. Their integration into buildings and infrastructure not only enhances energy management efficiency but also strengthens the stability of power systems, thereby driving society towards a more environmentally friendly and sustainable direction. This simultaneously establishes a solid foundation for the long-term stability of the supercapacitor industry, as shown in Fig. 26.

CRediT authorship contribution statement

Caiyu Zhao: Writing – review & editing, Writing – original draft, Methodology, Investigation, Formal analysis, Data curation. **Wenkui Dong:** Writing – review & editing, Writing – original draft, Validation, Supervision, Conceptualization. **T.M. Indra Mahlia:** Writing – review & editing, Writing – original draft, Validation. **Long Shi:** Writing – review & editing, Writing – original draft, Validation. **Kejin Wang:** Writing – review & editing, Writing – original draft, Validation. **Surendra P. Shah:** Validation, Writing – review & editing. **Wengui Li:** Writing – review & editing, Writing – original draft, Validation, Supervision, Resources, Conceptualization.

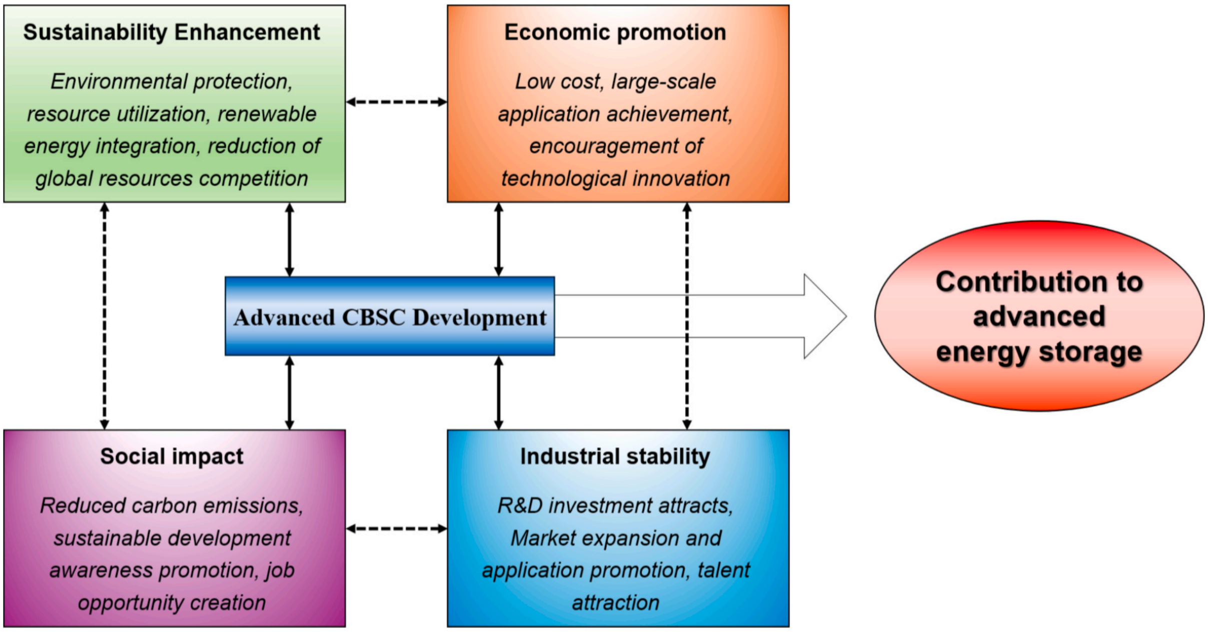

Fig. 26. Considerations for the development of CBSC to attain advanced energy storage [233].

Declaration of competing interest

The authors declare that they have no known competing financial interests or personal relationships that could have appeared to influence the work reported in this paper.

Acknowledgments

The authors acknowledge the support from the Australian Research Council (ARC), Australia (FT220100177, LP230100288, DP220101051, DP220100036; IH200100010). The first author also thanks the China Scholarship Council (CSC).

Data availability

Data will be made available on request.

References

[1] S. Bouckaert, A.F. Pales, C. McGlade, U. Remme, B. Wanner, L. Varro, D. D'Ambrosio, T. Spencer, Net zero by 2050: A roadmap for the global energy sector, (2021).
[2] Y.-M.C. R. Armstrong, Eds, The-Future-of-Energy-Storage, An Interdisciplinary MIT Study (MIT Energy Initiative, 2022).
[3] I.E. Agency, The role of critical minerals in clean energy transitions, part of world energy, Outlook (2021).
[4] J. Benedek, T.-T. Sebestyén, B. Bartók, Evaluation of renewable energy sources in peripheral areas and renewable energy-based rural development, Renew. Sustain. Energy Rev. 90 (2018) 516–535.
[5] J. Rissman, C. Bataille, E. Masanet, N. Aden, W.R. Morrow III, N. Zhou, N. Elliott, R. Dell, N. Heeren, B. Huckestein, Technologies and policies to decarbonize global industry: Review and assessment of mitigation drivers through 2070, Appl. Energy 266 (2020) 114848.
[6] P.D. Lund, J. Lindgren, J. Mikkola, J. Salpakari, Review of energy system flexibility measures to enable high levels of variable renewable electricity, Renew. Sustain. Energy Rev. 45 (2015) 785–807.
[7] X. Luo, D. Chung, Carbon-fiber/polymer-matrix composites as capacitors, Compos. Sci. Technol. 61 (6) (2001) 885–888.
[8] E.D. Wetzel, D.J. O'Brien, J.F. Snyder, R.H. Carter, J.T. South, Multifunctional structural power and energy composites for US army applications, Defence Technical Information Center: Fort Belvoir, VA, USA (2006).
[9] Q. Meng, D. Chung, Battery in the form of a cement-matrix composite, Cem. Concr. Compos. 32 (10) (2010) 829–839.
[10] J. Zhang, J. Xu, D. Zhang, A structural supercapacitor based on graphene and hardened cement paste, J. Electrochem. Soc. 163 (3) (2015) E83.
[11] Q. Zhao, S. Stalin, C.-Z. Zhao, L.A. Archer, Designing solid-state electrolytes for safe, energy-dense batteries, Nat. Rev. Mater. 5 (3) (2020) 229–252.
[12] J.F. Snyder, D.J. O'Brien, D.M. Baechle, D.E. Mattson, E.D. Wetzel, Structural composite capacitors, supercapacitors, and batteries for US Army Applications, 2008.
[13] T. Ye, L. Li, Y. Zhang, Recent progress in solid electrolytes for energy storage devices, Adv. Funct. Mater. 30 (29) (2020) 2000077.
[14] V. Kumaravel, J. Bartlett, S.C. Pillai, Solid electrolytes for high-temperature stable batteries and supercapacitors, Adv. Energy Mater. 11 (3) (2021) 2002869.
[15] W. Raza, F. Ali, N. Raza, Y. Luo, K.-H. Kim, J. Yang, S. Kumar, A. Mehmood, E. E. Kwon, Recent advancements in supercapacitor technology, Nano Energy 52 (2018) 441–473.
[16] F. Béguin, V. Presser, A. Balducci, E. Frackowiak, Carbons and electrolytes for advanced supercapacitors, Adv. Mater. 26 (14) (2014) 2219–2251.
[17] T. Famprikis, P. Canepa, J.A. Dawson, M.S. Islam, C. Masquelier, Fundamentals of inorganic solid-state electrolytes for batteries, Nat. Mater. 18 (12) (2019) 1278–1291.
[18] J. Wang, P. Zhan, D. Zhang, Redox active cement-based electrolyte towards high-voltage asymmetric solid supercapacitor, Cem. Concr. Compos. 138 (2023) 104987.
[19] H. Wang, L. Pilon, Accurate simulations of electric double layer capacitance of ultramicroelectrodes, J. Phys. Chem. C 115 (33) (2011) 16711–16719.
[20] K.-Y. Chan, B. Jia, H. Lin, N. Hameed, J.-H. Lee, K.-T. Lau, A critical review on multifunctional composites as structural capacitors for energy storage, Compos. Struct. 188 (2018) 126–142.
[21] A. Noori, M.F. El-Kady, M.S. Rahmanifar, R.B. Kaner, M.F. Mousavi, Towards establishing standard performance metrics for batteries, supercapacitors and beyond, Chem. Soc. Rev. 48 (5) (2019) 1272–1341.
[22] H.V. Helmholtz, Ueber einige Gesetze der Vertheilung elektrischer Ströme in körperlichen Leitern, mit Anwendung auf die thierisch-elektrischen Versuche (Schluss.),, Ann. Phys. 165 (7) (1853) 353–377.
[23] A.J. Bard, L.R. Faulkner, H.S. White, Electrochemical methods: fundamentals and applications, John Wiley & Sons, 2022.
[24] L.L. Zhang, X. Zhao, Carbon-based materials as supercapacitor electrodes, Chem. Soc. Rev. 38 (9) (2009) 2520–2531.
[25] X. Mao, P. Brown, C. Červinka, G. Hazell, H. Li, Y. Ren, D. Chen, R. Atkin, J. Eastoe, I. Grillo, Self-assembled nanostructures in ionic liquids facilitate charge storage at electrified interfaces, Nat. Mater. 18 (12) (2019) 1350–1357.
[26] D.L. Chapman, Li, A contribution to the theory of electrocapillarity, The London, Edinburgh, and Dublin Philosophical Magazine and Journal of, Science 25 (148) (1913) 475–481.
[27] M. Gouy, Sur la constitution de la charge électrique à la surface d'un électrolyte, J. Phys. Theor. Appl. 9 (1) (1910) 457–468.
[28] Y. Jiang, J. Liu, Definitions of pseudocapacitive materials: a brief review, Energy Environ. Mater. 2 (1) (2019) 30–37.
[29] R. Chen, M. Yu, R.P. Sahu, I.K. Puri, I. Zhitomirsky, The development of pseudocapacitor electrodes and devices with high active mass loading, Adv. Energy Mater. 10 (20) (2020) 1903848.
[30] P. Simon, Y. Gogotsi, Materials for electrochemical capacitors, Nat. Mater. 7 (11) (2008) 845–854.
[31] V. Augustyn, P. Simon, B. Dunn, Pseudocapacitive oxide materials for high-rate electrochemical energy storage, Energ. Environ. Sci. 7 (5) (2014) 1597–1614.
[32] C. Choi, D.S. Ashby, D.M. Butts, R.H. DeBlock, Q. Wei, J. Lau, B. Dunn, Achieving high energy density and high power density with pseudocapacitive materials, Nat. Rev. Mater. 5 (1) (2020) 5–19.

[33] S. Trasatti, G. Buzzanca, Ruthenium dioxide: A new interesting electrode material. Solid state structure and electrochemical behaviour, J. Electroanal. Chem. Interfacial Electrochem. 29 (2) (1971) A1–A5.
[34] P. Simon, Y. Gogotsi, Perspectives for electrochemical capacitors and related devices, Nat. Mater. 19 (11) (2020) 1151–1163.
[35] B.E. Conway, Electrochemical supercapacitors: scientific fundamentals and technological applications, Springer Science and Business Media, 2013.
[36] Y. Liu, S.P. Jiang, Z. Shao, Intercalation pseudocapacitance in electrochemical energy storage: recent advances in fundamental understanding and materials development, Mater. Today Adv. 7 (2020) 100072.
[37] B.-Y. Chang, E. Ahn, S.-M. Park, Real-time staircase cyclic voltammetry fourier transform electrochemical impedance spectroscopic studies on underpotential deposition of lead on gold, J. Phys. Chem. C 112 (43) (2008) 16902–16909.
[38] P. Simon, Y. Gogotsi, B. Dunn, Where do batteries end and supercapacitors begin? Science 343 (6176) (2014) 1210–1211.
[39] N. Chanut, D. Stefaniuk, J.C. Weaver, Y. Zhu, Y. Shao-Horn, A. Masic, F.-J. Ulm, Carbon–cement supercapacitors as a scalable bulk energy storage solution, Proc. Natl. Acad. Sci. 120 (32) (2023) e2304318120.
[40] S. Zhang, N. Pan, Supercapacitors performance evaluation, Adv. Energy Mater. 5 (6) (2015) 1401401.
[41] P. Taberna, P. Simon, J.-F. Fauvarque, Electrochemical characteristics and impedance spectroscopy studies of carbon-carbon supercapacitors, J. Electrochem. Soc. 150 (3) (2003) A292.
[42] M.F. Dupont, A.F. Hollenkamp, S.W. Donne, Large amplitude electrochemical impedance spectroscopy for characterizing the performance of electrochemical capacitors, J. Electrochem. Soc. 161 (4) (2014) A648.
[43] Y. Zhu, S. Murali, M.D. Stoller, K.J. Ganesh, W. Cai, P.J. Ferreira, A. Pirkle, R. M. Wallace, K.A. Cychosz, M. Thommes, Carbon-based supercapacitors produced by activation of graphene, Science 332 (6037) (2011) 1537–1541.
[44] P.A. Claisse, Civil engineering materials, Butterworth-Heinemann2015.
[45] Q. Zhao, J. Chen, F. Luo, L. Shen, Y. Wang, K. Wu, M. Lu, Vertically oriented polyaniline-graphene nanocomposite based on functionalized graphene for supercapacitor electrode, J. Appl. Polym. Sci. 134 (19) (2017).
[46] A.M. Navarro-Suárez, K.L. Van Aken, T. Mathis, T. Makaryan, J. Yan, J. Carretero-González, T. Rojo, Y. Gogotsi, Development of asymmetric supercapacitors with titanium carbide-reduced graphene oxide couples as electrodes, Electrochim. Acta 259 (2018) 752–761.
[47] M. Zhang, X. Yu, H. Ma, W. Du, L. Qu, C. Li, G. Shi, Robust graphene composite films for multifunctional electrochemical capacitors with an ultrawide range of areal mass loading toward high-rate frequency response and ultrahigh specific capacitance, Energ. Environ. Sci. 11 (3) (2018) 559–565.
[48] A. Oz, D. Gelman, E. Goren, N. Shomrat, S. Baltianski, Y. Tsur, A novel approach for supercapacitors degradation characterization, J. Power Sources 355 (2017) 74–82.
[49] F. Rafik, H. Gualous, R. Gallay, A. Crausaz, A. Berthon, Frequency, thermal and voltage supercapacitor characterization and modeling, J. Power Sources 165 (2) (2007) 928–934.
[50] D. Stevens, J. Dahn, The mechanisms of lithium and sodium insertion in carbon materials, J. Electrochem. Soc. 148 (8) (2001) A803.
[51] D. DiVincenzo, E. Mele, Cohesion and structure in stage-1 graphite intercalation compounds, Phys. Rev. B 32 (4) (1985) 2538.
[52] W. Xing, J. Dahn, Study of irreversible capacities for Li insertion in hard and graphitic carbons, J. Electrochem. Soc. 144 (4) (1997) 1195.
[53] X. Xia, M. Obrovac, J. Dahn, Comparison of the reactivity of NaxC6 and LixC6 with non-aqueous solvents and electrolytes, Electrochem. Solid St. 14 (9) (2011) A130.
[54] J. Auvergniot, A. Cassel, J.-B. Ledeuil, V. Viallet, V. Seznec, R. Dedryvère, Interface stability of argyrodite Li6PS5Cl toward LiCoO2, LiNi1/3Co1/3Mn1/3O2, and LiMn2O4 in bulk all-solid-state batteries, Chem. Mater. 29 (9) (2017) 3883–3890.
[55] H.J. Lee, X. Liu, Y. Chart, P. Tang, J.-G. Bae, S. Narayanan, J.H. Lee, R.J. Potter, Y. Sun, M. Pasta, LiNi0. 5Mn1. 5O4 cathode microstructure for all-solid-state batteries, Nano Letters 22(18) (2022) 7477-7483.
[56] J. Janek, W.G. Zeier, Challenges in speeding up solid-state battery development, Nat. Energy 8 (3) (2023) 230–240.
[57] C. Fang, D. Zhang, A large areal capacitance structural supercapacitor with a 3D rGO@ MnO 2 foam electrode and polyacrylic acid–Portland cement–KOH electrolyte, J. Mater. Chem. A 8 (25) (2020) 12586–12593.
[58] J. Wang, D. Zhang, Structural supercapacitor constructed by SnO2/graphene coated nickel foam electrode and synchronously synthesized polymer cement electrolyte at room temperature, Mater. Chem. Phys. 277 (2022) 125488.
[59] P. Jiao, C. Fang, D. Zhang, In-situ polymerized polyacrylamide/magnesium phosphate cement electrolyte for structural supercapacitor, J. Storage Mater. 55 (2022) 105416.
[60] S. Zhu, Y. Sun, K. Li, Y. Dang, X. Guan, Construction of structural supercapacitor with high energy density and mechanical strength based on dual-carbon electrodes and polyacrylamide-Portland cement-Na2SO4 electrolyte, J. Power Sources 597 (2024) 234150.
[61] J. Wang, P. Zhan, D. Zhang, L. Tang, Nickel cobalt sulfide composite nanosheet anchored on rGO as effective electrode for quasi-solid supercapacitor, J. Storage Mater. 70 (2023) 107938.
[62] M.J. Wang, R. Choudhury, J. Sakamoto, Characterizing the Li-solid-electrolyte interface dynamics as a function of stack pressure and current density, Joule 3 (9) (2019) 2165–2178.
[63] B.E. Francisco, C.R. Stoldt, J.-C. M`Peko, Lithium-ion trapping from local structural distortions in sodium super ionic conductor (NASICON) electrolytes, Chem. Mater. 26 (16) (2014) 4741–4749.
[64] X. He, Y. Zhu, Y. Mo, Origin of fast ion diffusion in super-ionic conductors, Nat. Commun. 8 (1) (2017) 15893.
[65] F. Moccia, Q. Yu, M. Fernández Ruiz, A. Muttoni, Concrete compressive strength: From material characterization to a structural value, Struct. Concr. 22 (2021) E634–E654.
[66] J. Del Viso, J. Carmona, G. Ruiz, Shape and size effects on the compressive strength of high-strength concrete, Cem. Concr. Res. 38 (3) (2008) 386–395.
[67] C. Prehal, D. Weingarth, E. Perre, R.T. Lechner, H. Amenitsch, O. Paris, V. Presser, Tracking the structural arrangement of ions in carbon supercapacitor nanopores using in situ small-angle X-ray scattering, Energ. Environ. Sci. 8 (6) (2015) 1725–1735.
[68] B.E. Conway, V. Birss, J. Wojtowicz, The role and utilization of pseudocapacitance for energy storage by supercapacitors, J. Power Sources 66 (1–2) (1997) 1–14.
[69] M. Toupin, T. Brousse, D. Bélanger, Charge storage mechanism of MnO2 electrode used in aqueous electrochemical capacitor, Chem. Mater. 16 (16) (2004) 3184–3190.
[70] A. Allagui, T.J. Freeborn, A.S. Elwakil, B.J. Maundy, Reevaluation of performance of electric double-layer capacitors from constant-current charge/discharge and cyclic voltammetry, Sci. Rep. 6 (1) (2016) 38568.
[71] X. Pu, D. Zhao, C. Fu, Z. Chen, S. Cao, C. Wang, Y. Cao, Understanding and calibration of charge storage mechanism in cyclic voltammetry curves, Angew. Chem. Int. Ed. 60 (39) (2021) 21310–21318.
[72] D.M. Morales, M. Risch, Seven steps to reliable cyclic voltammetry measurements for the determination of double layer capacitance, Journal of Physics: Energy 3 (3) (2021) 034013.
[73] M.D. Stoller, R.S. Ruoff, Best practice methods for determining an electrode material`s performance for ultracapacitors, Energ. Environ. Sci. 3 (9) (2010) 1294–1301.
[74] Y. Gogotsi, P. Simon, True performance metrics in electrochemical energy storage, Science 334 (6058) (2011) 917–918.
[75] J. Chmiola, C. Largeot, P.-L. Taberna, P. Simon, Y. Gogotsi, Monolithic carbide-derived carbon films for micro-supercapacitors, Science 328 (5977) (2010) 480–483.
[76] J.R. Miller, R. Outlaw, B. Holloway, Graphene double-layer capacitor with ac line-filtering performance, Science 329 (5999) (2010) 1637–1639.
[77] C. Du, N. Pan, Supercapacitors using carbon nanotubes films by electrophoretic deposition, J. Power Sources 160 (2) (2006) 1487–1494.
[78] D.K. Kampouris, X. Ji, E.P. Randviir, C.E. Banks, A new approach for the improved interpretation of capacitance measurements for materials utilised in energy storage, RSC Adv. 5 (17) (2015) 12782–12791.
[79] K. Subramani, N. Sudhan, R. Divya, M. Sathish, All-solid-state asymmetric supercapacitors based on cobalt hexacyanoferrate-derived CoS and activated carbon, RSC Adv. 7 (11) (2017) 6648–6659.
[80] J. Yan, T. Wei, B. Shao, F. Ma, Z. Fan, M. Zhang, C. Zheng, Y. Shang, W. Qian, F. Wei, Electrochemical properties of graphene nanosheet/carbon black composites as electrodes for supercapacitors, Carbon 48 (6) (2010) 1731–1737.
[81] M. Lu, Supercapacitors: materials, systems, and applications, John Wiley & Sons, 2013.
[82] M. Schneider, M. Romer, M. Tschudin, H. Bolio, Sustainable cement production—present and future, Cem. Concr. Res. 41 (7) (2011) 642–650.
[83] A. Rahman, V. Srikumar, A.D. Smith, Predicting electricity consumption for commercial and residential buildings using deep recurrent neural networks, Appl. Energy 212 (2018) 372–385.
[84] T. Huo, H. Ren, X. Zhang, W. Cai, W. Feng, N. Zhou, X. Wang, China's energy consumption in the building sector: A Statistical Yearbook-Energy Balance Sheet based splitting method, J. Clean. Prod. 185 (2018) 665–679.
[85] W. Ma, D. Zhang, Multifunctional structural supercapacitor based on graphene and magnesium phosphate cement, J. Compos. Mater. 53 (6) (2019) 719–730.
[86] J. Tu, X. Chen, X. Xiong, Y. Chen, J. Ma, H. Cao, A. Li, Microwave hydrothermal electrodeposition of nickel carbonate hydroxide/cobalt hydroxide film on nickel foam for cement-based structural supercapacitors, Mater. Today Chem. 28 (2023) 101365.
[87] D. Madej, K. Sieroń, A. Kruk, Synthesis and performance of aluminous cements containing zirconium and strontium as alternatives to the calcium aluminate cements designed for the production of high performance refractories, Cem. Concr. Compos. 130 (2022) 104518.
[88] B. Pal, S. Yang, S. Ramesh, V. Thangadurai, R. Jose, Electrolyte selection for supercapacitive devices: a critical review, Nanoscale Adv. 1 (10) (2019) 3807–3835.
[89] W. Ru, Y. Lijuan, W. Peiming, Recent research development on mechanism of polymer modification to cement-based materials, Bulletin of the Chinese Ceramic Society 30 (4) (2011) 818–821.
[90] Y. Qiao, On the fracture toughness of calcium aluminate cement–phenol resin composites, Cem. Concr. Res. 35 (2) (2005) 220–225.
[91] E. Sakai, J. Sugita, Composite mechanism of polymer modified cement, Cem. Concr. Res. 25 (1) (1995) 127–135.
[92] A.A. Bonapasta, F. Buda, P. Colombet, G. Guerrini, Cross-linking of poly (vinyl alcohol) chains by Ca ions in macro-defect-free cements, Chem. Mater. 14 (3) (2002) 1016–1022.
[93] P. Tomar, R. Lakhani, V. Chhibber, R. Kumar, Macro-defect free cements: a future oriented polymer composite materials for construction industries, Compos. Interfaces 25 (5–7) (2018) 607–627.

[94] M. Delucchi, G. Cerisola, Influence of organic coatings on the stability of macrodefect-free cements exposed to water, Constr. Build. Mater. 15 (7) (2001) 351–359.

[95] G. Merle, S.S. Hosseiny, M. Wessling, K. Nijmeijer, New cross-linked PVA based polymer electrolyte membranes for alkaline fuel cells, J. Membr. Sci. 409 (2012) 191–199.

[96] C. Xu, D. Zhang, Multifunctional structural supercapacitor based on cement/PVA-KOH composite and graphene, J. Compos. Mater. 55 (10) (2021) 1359–1369.

[97] Y. Zhang, D. Zhang, High areal capacitance nickel-cobalt transition metal hydroxide/reduced graphene for structural supercapacitors, Electrochim. Acta 475 (2024) 143591.

[98] N. Shi, D. Zhang, Inorganic-organic composite solid electrolyte based on cement and Polyacrylamide prepared by a synchronous reaction method, Electrochim. Acta 391 (2021) 138998.

[99] S.-Y. Guo, X. Zhang, J.-Z. Chen, B. Mou, H.-S. Shang, P. Wang, L. Zhang, J. Ren, Mechanical and interface bonding properties of epoxy resin reinforced Portland cement repairing mortar, Constr. Build. Mater. 264 (2020) 120715.

[100] C. Fang, D. Zhang, High multifunctional performance structural supercapacitor with Polyethylene oxide cement electrolyte and reduced graphene oxide@ CuCo2O4 nanowires, Electrochim. Acta 401 (2022) 139491.

[101] C. Fang, D. Zhang, High areal energy density structural supercapacitor assembled with polymer cement electrolyte, Chem. Eng. J. 426 (2021) 130793.

[102] C. Pei, T. Ueda, J. Zhu, Investigation of the effectiveness of graphene/polyvinyl alcohol on the mechanical and electrical properties of cement composites, Mater. Struct. 53 (2020) 1–15.

[103] P. Dong, M.R. Ahmad, B. Chen, M.J. Munir, S.M.S. Kazmi, A study on magnesium phosphate cement mortars reinforced by polyvinyl alcohol fibers, Constr. Build. Mater. 302 (2021) 124154.

[104] J. Wang, C. Xu, D. Zhang, P. Zhan, Porous polymer cement composites for quasi-solid graphene supercapacitors, J. Storage Mater. 63 (2023) 106991.

[105] C. Gelfi, P.G. Righetti, Polymerization kinetics of polyacrylamide gels I, Effect of Different Cross-linkers, Electrophoresis 2 (4) (1981) 213–219.

[106] C. Gelfi, P.G. Righetti, Polymerization kinetics of polyacrylamide gels II, Effect of Temperature, Electrophoresis 2 (4) (1981) 220–228.

[107] J.-H. Kim, R.E. Robertson, Prevention of air void formation in polymer-modified cement mortar by pre-wetting, Cem. Concr. Res. 27 (2) (1997) 171–176.

[108] J.-H. Kim, R.E. Robertson, Effects of polyvinyl alcohol on aggregate-paste bond strength and the interfacial transition zone, Adv. Cem. Bas. Mat. 8 (2) (1998) 66–76.

[109] A. Allahverdi, K. Kianpur, M. Moghbeli, Effect of polyvinyl alcohol on flexural strength and some important physical properties of Portland cement paste, Iran. J. Mater. Sci. Eng 7 (1) (2010) 1–6.

[110] C. Gao, J. Tang, Z. Meng, Y. Chu, J. Huang, F. Han, J. Liu, Enhancement in toughness of cement pastes by chitosan modified with polyacrylic acid (CS/PAA): Microstructure evolution and molecular dynamics, Journal of Building Engineering 79 (2023) 107822.

[111] R. Liang, Q. Liu, D. Hou, Z. Li, G. Sun, Flexural strength enhancement of cement paste through monomer incorporation and in situ bond formation, Cem. Concr. Res. 152 (2022) 106675.

[112] Q. Yuan, Z. Xie, H. Yao, T. Huang, M. Fan, Hydration, mechanical properties, and microstructural characteristics of cement pastes with different ionic polyacrylamides: A comparative study, Journal of Building Engineering 56 (2022) 104763.

[113] J. Hu, D. Koleva, Y. Ma, E. Schlangen, P. Petrov, K. Van Breugel, The influence of admixed micelles on the microstructural properties and global performance of cement-based materials, Cem. Concr. Res. 42 (8) (2012) 1122–1133.

[114] C.-Z. Li, N.-Q. Feng, R.-J. Chen, Effects of polyethlene oxide chains on the performance of polycarboxylate-type water-reducers, Cement and Concrete Cesearch 35 (5) (2005) 867–873.

[115] L. Yin, S. Liu, D. Yin, K. Du, J. Yan, C.K. Armwood-Gordon, L. Li, Development of rechargeable cement-based batteries with carbon fiber mesh for energy storage solutions, J. Storage Mater. 93 (2024) 112181.

[116] A. Sedaghat, M.K. Ram, A. Zayed, R. Kamal, N. Shanahan, Investigation of physical properties of graphene-cement composite for structural applications, Open Journal of Composite Materials 2014 (2014).

[117] C. Tang, K. Hackenberg, Q. Fu, P.M. Ajayan, H. Ardebili, High ion conducting polymer nanocomposite electrolytes using hybrid nanofillers, Nano Lett. 12 (3) (2012) 1152–1156.

[118] G. Ma, J. Li, K. Sun, H. Peng, J. Mu, Z. Lei, High performance solid-state supercapacitor with PVA–KOH–K3 [Fe (CN) 6] gel polymer as electrolyte and separator, J. Power Sources 256 (2014) 281–287.

[119] J.F. Snyder, R.H. Carter, E.D. Wetzel, Electrochemical and mechanical behavior in mechanically robust solid polymer electrolytes for use in multifunctional structural batteries, Chem. Mater. 19 (15) (2007) 3793–3801.

[120] R. Agrawal, G. Pandey, Solid polymer electrolytes: materials designing and all-solid-state battery applications: an overview, J. Phys. D Appl. Phys. 41 (22) (2008) 223001.

[121] A. Lewandowski, M. Zajder, E. Frąckowiak, F. Beguin, Supercapacitor based on activated carbon and polyethylene oxide–KOH–H2O polymer electrolyte, Electrochim. Acta 46 (18) (2001) 2777–2780.

[122] Q. Li, Z. Dai, J. Wu, W. Liu, T. Di, R. Jiang, X. Zheng, W. Wang, X. Ji, P. Li, Fabrication of ordered macro-microporous single-crystalline MOF and its derivative carbon material for supercapacitor, Adv. Energy Mater. 10 (33) (2020) 1903750.

[123] P. Zhan, J. Xu, J. Wang, J. Zuo, Z. He, Structural supercapacitor electrolytes based on cementitious composites containing recycled steel slag and waste glass powders, Cem. Concr. Compos. 137 (2023) 104924.

[124] Y. Matsuda, H. Nakashima, M. Morita, Y. Takasu, Behavior of some ions in mixed organic electrolytes of high energy density batteries, J. Electrochem. Soc. 128 (12) (1981) 2552.

[125] S. Dhir, S. Wheeler, I. Capone, M. Pasta, Outlook on K-ion batteries, Chem 6 (10) (2020) 2442–2460.

[126] T. Hosaka, K. Kubota, H. Kojima, S. Komaba, Highly concentrated electrolyte solutions for 4 V class potassium-ion batteries, Chem. Commun. 54 (60) (2018) 8387–8390.

[127] S. Dhir, B. Jagger, A. Maguire, M. Pasta, Fundamental investigations on the ionic transport and thermodynamic properties of non-aqueous potassium-ion electrolytes, Nat. Commun. 14 (1) (2023) 3833.

[128] M. Okoshi, Y. Yamada, S. Komaba, A. Yamada, H. Nakai, Theoretical analysis of interactions between potassium ions and organic electrolyte solvents: a comparison with lithium, sodium, and magnesium ions, J. Electrochem. Soc. 164 (2) (2016) A54.

[129] C. Largeot, C. Portet, J. Chmiola, P.-L. Taberna, Y. Gogotsi, P. Simon, Relation between the ion size and pore size for an electric double-layer capacitor, J. Am. Chem. Soc. 130 (9) (2008) 2730–2731.

[130] M. Hashemi, M.S. Rahmanifar, M.F. El-Kady, A. Noori, M.F. Mousavi, R.B. Kaner, The use of an electrocatalytic redox electrolyte for pushing the energy density boundary of a flexible polyaniline electrode to a new limit, Nano Energy 44 (2018) 489–498.

[131] I. Shown, A. Ganguly, L.C. Chen, K.H. Chen, Conducting polymer-based flexible supercapacitor, Energy Sci. Eng. 3 (1) (2015) 2–26.

[132] Y. Luo, W. Hong, Z. Xiao, H. Bai, A high-performance electrochemical supercapacitor based on a polyaniline/reduced graphene oxide electrode and a copper (ii) ion active electrolyte, PCCP 20 (1) (2018) 131–136.

[133] W. Liu, S. Zhang, S.U. Dar, Y. Zhao, R. Akram, X. Zhang, S. Jin, Z. Wu, D. Wu, Polyphosphazene-derived heteroatoms-doped carbon materials for supercapacitor electrodes, Carbon 129 (2018) 420–427.

[134] N. Job, A. Théry, R. Pirard, J. Marien, L. Kocon, J.-N. Rouzaud, F. Béguin, J.-P. Pirard, Carbon aerogels, cryogels and xerogels: Influence of the drying method on the textural properties of porous carbon materials, Carbon 43 (12) (2005) 2481–2494.

[135] E. Raymundo-Piñero, M. Cadek, F. Béguin, Tuning carbon materials for supercapacitors by direct pyrolysis of seaweeds, Adv. Funct. Mater. 19 (7) (2009) 1032–1039.

[136] E. Frackowiak, F. Beguin, Carbon materials for the electrochemical storage of energy in capacitors, Carbon 39 (6) (2001) 937–950.

[137] D. Sheberla, J.C. Bachman, J.S. Elias, C.-J. Sun, Y. Shao-Horn, M. Dincă, Conductive MOF electrodes for stable supercapacitors with high areal capacitance, Nat. Mater. 16 (2) (2017) 220–224.

[138] A. Burke, R&D considerations for the performance and application of electrochemical capacitors, Electrochim. Acta 53 (3) (2007) 1083–1091.

[139] J. Chmiola, G. Yushin, Y. Gogotsi, C. Portet, P. Simon, P.-L. Taberna, Anomalous increase in carbon capacitance at pore sizes less than 1 nanometer, Science 313 (5794) (2006) 1760–1763.

[140] T. Centeno, F. Stoeckli, Surface-related capacitance of microporous carbons in aqueous and organic electrolytes, Electrochim. Acta 56 (21) (2011) 7334–7339.

[141] W. Gu, G. Yushin, Review of nanostructured carbon materials for electrochemical capacitor applications: advantages and limitations of activated carbon, carbide-derived carbon, zeolite-templated carbon, carbon aerogels, carbon nanotubes, onion-like carbon, and graphene, Wiley Interdiscip. Rev.: Energy Environ. 3 (5) (2014) 424–473.

[142] A. Izadi-Najafabadi, S. Yasuda, K. Kobashi, T. Yamada, D.N. Futaba, H. Hatori, M. Yumura, S. Iijima, K. Hata, Extracting the full potential of single-walled carbon nanotubes as durable supercapacitor electrodes operable at 4 V with high power and energy density, Adv. Mater. 22 (35) (2010) E235–E241.

[143] L. Zhang, F. Zhang, X. Yang, G. Long, Y. Wu, T. Zhang, K. Leng, Y. Huang, Y. Ma, A. Yu, Porous 3D graphene-based bulk materials with exceptional high surface area and excellent conductivity for supercapacitors, Sci. Rep. 3 (1) (2013) 1408.

[144] Y. Xu, Z. Lin, X. Zhong, X. Huang, N.O. Weiss, Y. Huang, X. Duan, Holey graphene frameworks for highly efficient capacitive energy storage, Nat. Commun. 5 (1) (2014) 4554.

[145] X. Yang, C. Cheng, Y. Wang, L. Qiu, D. Li, Liquid-mediated dense integration of graphene materials for compact capacitive energy storage, Science 341 (6145) (2013) 534–537.

[146] C. Fang, D. Zhang, Portland cement electrolyte for structural supercapacitor in building application, Constr. Build. Mater. 285 (2021) 122897.

[147] C. Fang, D. Zhang, Enhanced Electrochemical Matching between NiCo2O4/ Reduced Graphene Oxide and Polymer Cement Electrolyte for Structural Supercapacitor, J. Electrochem. Soc. 169 (6) (2022) 060528.

[148] Y. Zhang, D. Zhang, Enhanced all-solid-state structural supercapacitor performance of rGO/N1C1M-S3'nanosheets with high areal capacitance, J. Alloy. Compd. 968 (2023) 172099.

[149] E. Hu, Y. Feng, J. Nai, D. Zhao, Y. Hu, X.W.D. Lou, Construction of hierarchical Ni–Co–P hollow nanobricks with oriented nanosheets for efficient overall water splitting, Energ. Environ. Sci. 11 (4) (2018) 872–880.

[150] A.C. Luntz, J. Voss, K. Reuter, Interfacial challenges in solid-state Li ion batteries, ACS Publications (2015) 4599–4604.

[151] J. Haruyama, K. Sodeyama, L. Han, K. Takada, Y. Tateyama, Space–charge layer effect at interface between oxide cathode and sulfide electrolyte in all-solid-state lithium-ion battery, Chem. Mater. 26 (14) (2014) 4248–4255.

[152] N.J. de Klerk, M. Wagemaker, Space-charge layers in all-solid-state batteries; important or negligible? ACS Appl. Energy Mater. 1 (10) (2018) 5609–5618.
[153] S. Dai, B. Zhao, C. Qu, D. Chen, D. Dang, B. Song, B.M. Deglee, J. Fu, C. Hu, C.-P. Wong, Controlled synthesis of three-phase NixSy/rGO nanoflake electrodes for hybrid supercapacitors with high energy and power density, Nano Energy 33 (2017) 522–531.
[154] T. Zhao, W. Yang, X. Zhao, X. Peng, J. Hu, C. Tang, T. Li, Facile preparation of reduced graphene oxide/copper sulfide composite as electrode materials for supercapacitors with high energy density, Compos. B Eng. 150 (2018) 60–67.
[155] K. Yang, K. Cho, S. Kim, Effect of carbon black addition on thermal stability and capacitive performances of supercapacitors, Sci. Rep. 8 (1) (2018) 11989.
[156] Y. Wang, J. Guo, T. Wang, J. Shao, D. Wang, Y.-W. Yang, Mesoporous transition metal oxides for supercapacitors, Nanomaterials 5 (4) (2015) 1667–1689.
[157] S. Chen, J. Zhu, X. Wu, Q. Han, X. Wang, Graphene oxide− MnO2 nanocomposites for supercapacitors, ACS Nano 4 (5) (2010) 2822–2830.
[158] Y. Zhou, P. Jin, Y. Zhou, Y. Zhu, High-performance symmetric supercapacitors based on carbon nanotube/graphite nanofiber nanocomposites, Sci. Rep. 8 (1) (2018) 9005.
[159] Q. Wu, T. He, Y. Zhang, J. Zhang, Z. Wang, Y. Liu, L. Zhao, Y. Wu, F. Ran, Cyclic stability of supercapacitors: materials, energy storage mechanism, test methods, and device, J. Mater. Chem. A 9 (43) (2021) 24094–24147.
[160] V.S. Devi, M. Athika, E. Duraisamy, A. Prasath, A.S. Sharma, P. Elumalai, Facile sol-gel derived nanostructured spinel Co3O4 as electrode material for high-performance supercapattery and lithium-ion storage, J. Storage Mater. 25 (2019) 100815.
[161] P. Ragupathy, D.H. Park, G. Campet, H. Vasan, S.-J. Hwang, J.-H. Choy, N. Munichandraiah, Remarkable capacity retention of nanostructured manganese oxide upon cycling as an electrode material for supercapacitor, J. Phys. Chem. C 113 (15) (2009) 6303–6309.
[162] S. Fleischmann, M. Widmaier, A. Schreiber, H. Shim, F.M. Stiemke, T.J. Schubert, V. Presser, High voltage asymmetric hybrid supercapacitors using lithium-and sodium-containing ionic liquids, Energy Storage Mater. 16 (2019) 391–399.
[163] L. Christodoulou, J.D. Venables, Multifunctional material systems: The first generation, JOM 55 (2003) 39–45.
[164] L.E. Asp, Multifunctional composite materials for energy storage in structural load paths, Plast., Rubber Compos. 42 (4) (2013) 144–149.
[165] M. Shi, D. Zhang, 3D Porous cementitious electrolyte with "stream-reservoir" ionic channels for high multifunctional performance structural supercapacitors, J. Mater. Chem. A (2024).
[166] H. Li, X. Wang, W. Jiang, H. Fu, X. Liang, K. Zhang, Z. Li, C. Zhao, H. Feng, J. Nie, Alkali Metal Chlorides Based Hydrogel as Eco-Friendly Neutral Electrolyte for Bendable Solid-State Capacitor, Adv. Mater. Interfaces 5 (10) (2018) 1701648.
[167] W. Li, Y. Guo, X. Zhang, W. Dong, X. Li, T. Yu, K. Wang, Development of self-sensing ultra-high-performance concrete using hybrid carbon black and carbon nanofibers, Cem. Concr. Compos. 105466 (2024).
[168] Y. Guo, W. Li, W. Dong, Z. Luo, F. Qu, F. Yang, K. Wang, Self-sensing performance of cement-based sensor with carbon black and polypropylene fibre subjected to different loading conditions, Journal of Building Engineering 59 (2022) 105003.
[169] Y. Guo, W. Li, W. Dong, K. Wang, X. He, K. Vessalas, D. Sheng, Self-sensing cement-based sensors with superhydrophobic and self-cleaning capacities after silane-based surficial treatments, Case Stud. Constr. Mater. 17 (2022) e01311.
[170] W. Li, W. Dong, Y. Guo, K. Wang, S.P. Shah, Advances in multifunctional cementitious composites with conductive carbon nanomaterials for smart infrastructure, Cem. Concr. Compos. 128 (2022) 104454.
[171] W. Dong, W. Li, Z. Luo, Y. Guo, K. Wang, Effect of layer-distributed carbon nanotube (CNT) on mechanical and piezoresistive performance of intelligent cement-based sensor, Nanotechnology 31 (50) (2020) 505503.
[172] W. Dong, W. Li, Y. Guo, X. He, D. Sheng, Effects of silica fume on physicochemical properties and piezoresistivity of intelligent carbon black-cementitious composites, Constr. Build. Mater. 259 (2020) 120399.
[173] F. Ubertini, S. Laflamme, H. Ceylan, A.L. Materazzi, G. Cerni, H. Saleem, A. D'Alessandro, A. Corradini, Novel nanocomposite technologies for dynamic monitoring of structures: a comparison between cement-based embeddable and soft elastomeric surface sensors, Smart Mater. Struct. 23 (4) (2014) 045023.
[174] Z. Deng, A.H. Mahmood, W. Dong, D. Sheng, X. Lin, W. Li, Piezoresistive performance of self-sensing bitumen emulsion-cement mortar with multi-walled carbon nanotubes, Cem. Concr. Compos. 153 (2024) 105718.
[175] R. Banerjee, A. Gebrekrstos, J.T. Orasugh, S.S. Ray, Nanocarbon-containing polymer composite foams: a review of systems for applications in electromagnetic interference shielding energy storage, and piezoresistive sensors, Ind. Eng. Chem. Res. 62 (18) (2023) 6807–6842.
[176] A.D.B. Ferreira, P.R. Nóvoa, A.T. Marques, Multifunctional material systems: a state-of-the-art review, Compos. Struct. 151 (2016) 3–35.
[177] Y. Shao, M.F. El-Kady, J. Sun, Y. Li, Q. Zhang, M. Zhu, H. Wang, B. Dunn, R. B. Kaner, Design and mechanisms of asymmetric supercapacitors, Chem. Rev. 118 (18) (2018) 9233–9280.
[178] M. Ran, J. Wang, D. Zhang, A superior electrolyte composite with high conductivity and strength based on alkali-activated slag and polyacrylamide for structural supercapacitor, J. Storage Mater. 79 (2024) 110169.
[179] R.O. Ritchie, The conflicts between strength and toughness, Nat. Mater. 10 (11) (2011) 817–822.
[180] S. Wang, M.W. Urban, Self-healing polymers, Nat. Rev. Mater. 5 (8) (2020) 562–583.
[181] Y. Yang, M.W. Urban, Self-healing polymeric materials, Chem. Soc. Rev. 42 (17) (2013) 7446–7467.
[182] S. Billiet, X.K. Hillewaere, R.F. Teixeira, F.E. Du Prez, Chemistry of crosslinking processes for self-healing polymers, Macromol. Rapid Commun. 34 (4) (2013) 290–309.
[183] J. Chen, F. Li, Y. Luo, Y. Shi, X. Ma, M. Zhang, D. Boukhvalov, Z. Luo, A self-healing elastomer based on an intrinsic non-covalent cross-linking mechanism, J. Mater. Chem. A 7 (25) (2019) 15207–15214.
[184] J. Han, H. Wang, Y. Yue, C. Mei, J. Chen, C. Huang, Q. Wu, X. Xu, A self-healable and highly flexible supercapacitor integrated by dynamically cross-linked electro-conductive hydrogels based on nanocellulose-templated carbon nanotubes embedded in a viscoelastic polymer network, Carbon 149 (2019) 1–18.
[185] Y. Huang, M. Zhong, Y. Huang, M. Zhu, Z. Pei, Z. Wang, Q. Xue, X. Xie, C. Zhi, A self-healable and highly stretchable supercapacitor based on a dual crosslinked polyelectrolyte, Nat. Commun. 6 (1) (2015) 10310.
[186] H. Wang, Y. Diao, Y. Lu, H. Yang, Q. Zhou, K. Chrulski, J.M. D'Arcy, Energy storing bricks for stationary PEDOT supercapacitors, Nat. Commun. 11 (1) (2020) 1–9.
[187] E.Q. Zhang, L. Tang, Rechargeable concrete battery, Buildings 11 (3) (2021) 103.
[188] J. Ruan, J. Zheng, L. Dong, R. Qiu, Environment-friendly technology of recovering full resources of waste capacitors, ACS Sustain. Chem. Eng. 5 (1) (2017) 287–293.
[189] X. Yang, F. Zhang, L. Zhang, T. Zhang, Y. Huang, Y. Chen, A high-performance graphene oxide-doped ion gel as gel polymer electrolyte for all-solid-state supercapacitor applications, Adv. Funct. Mater. 23 (26) (2013) 3353–3360.
[190] H. Dai, G. Zhang, D. Rawach, C. Fu, C. Wang, X. Liu, M. Dubois, C. Lai, S. Sun, Polymer gel electrolytes for flexible supercapacitors: Recent progress, challenges, and perspectives, Energy Storage Mater. 34 (2021) 320–355.
[191] W. Dong, J. Tang, K. Wang, Y. Huang, S.P. Shah, W. Li, Cement-based batteries for renewable and sustainable energy storage toward an energy-efficient future, Energy 134382 (2025).
[192] R. He, H. Ma, R.B. Hafiz, C. Fu, X. Jin, J. He, Determining porosity and pore network connectivity of cement-based materials by a modified non-contact electrical resistivity measurement: Experiment and theory, Mater. Des. 156 (2018) 82–92.
[193] D. Chung, Electrically conductive cement-based materials, Adv. Cem. Res. 16 (4) (2004) 167–176.
[194] E. Kamseu, M.C. Bignozzi, U. Melo, C. Leonelli, V.M. Sglavo, Design of inorganic polymer cements: Effects of matrix strengthening on microstructure, Constr. Build. Mater. 38 (2013) 1135–1145.
[195] G.G. Jang, B. Song, K.-S. Moon, C.-P. Wong, J.K. Keum, M.Z. Hu, Particle size effect in porous film electrodes of ligand-modified graphene for enhanced supercapacitor performance, Carbon 119 (2017) 296–304.
[196] A.G. Pandolfo, A.F. Hollenkamp, Carbon properties and their role in supercapacitors, J. Power Sources 157 (1) (2006) 11–27.
[197] W. Zhang, D. Schröder, T. Arlt, I. Manke, R. Koerver, R. Pinedo, D.A. Weber, J. Sann, W.G. Zeier, J. Janek, (Electro) chemical expansion during cycling: monitoring the pressure changes in operating solid-state lithium batteries, J. Mater. Chem. A 5 (20) (2017) 9929–9936.
[198] R. Koerver, W. Zhang, L. de Biasi, S. Schweidler, A.O. Kondrakov, S. Kolling, T. Brezesinski, P. Hartmann, W.G. Zeier, J. Janek, Chemo-mechanical expansion of lithium electrode materials–on the route to mechanically optimized all-solid-state batteries, Energ. Environ. Sci. 11 (8) (2018) 2142–2158.
[199] R. Koerver, I. Aygün, T. Leichtweiß, C. Dietrich, W. Zhang, J.O. Binder, P. Hartmann, W.G. Zeier, J.R. Janek, Capacity fade in solid-state batteries: interphase formation and chemomechanical processes in nickel-rich layered oxide cathodes and lithium thiophosphate solid electrolytes, Chem. Mater. 29 (13) (2017) 5574–5582.
[200] G. Bucci, B. Talamini, A.R. Balakrishna, Y.-M. Chiang, W.C. Carter, Mechanical instability of electrode-electrolyte interfaces in solid-state batteries, Phys. Rev. Mater. 2 (10) (2018) 105407.
[201] L. Phor, A. Kumar, S. Chahal, Electrode materials for supercapacitors: A comprehensive review of advancements and performance, J. Storage Mater. 84 (2024) 110698.
[202] N. Baig, M. Sajid, T.A. Saleh, Recent trends in nanomaterial-modified electrodes for electroanalytical applications, TrAC Trends Anal. Chem. 111 (2019) 47–61.
[203] K.S. Kumar, N. Choudhary, Y. Jung, J. Thomas, Recent advances in two-dimensional nanomaterials for supercapacitor electrode applications, ACS Energy Lett. 3 (2) (2018) 482–495.
[204] A. Kanwade, P.M. Shirage, A review on synergy of transition metal oxide nanostructured materials: Effective and coherent choice for supercapacitor electrodes, J. Storage Mater. 55 (2022) 105692.
[205] Z. Li, K. Xu, Y. Pan, Recent development of supercapacitor electrode based on carbon materials, Nanotechnol. Rev. 8 (1) (2019) 35–49.
[206] L. Zhang, F. Zhang, X. Yang, K. Leng, Y. Huang, Y. Chen, High-performance supercapacitor electrode materials prepared from various pollens, Small 9 (8) (2013) 1342–1347.
[207] W. Dong, S. Gao, S. Peng, L. Shi, S.P. Shah, W. Li, Graphene reinforced cement-based triboelectric nanogenerator for efficient energy harvesting in civil infrastructure, Nano Energy 131 (2024) 110380.
[208] W. Dong, S. Peng, K. Wang, Y. Huang, L. Shi, F. Wu, W. Li, Integrated triboelectric self-powering and piezoresistive self-sensing cementitious composites for intelligent civil infrastructure, Nano Energy 135 (2025) 110656.
[209] Y. Xu, W. Lu, G. Xu, T.-W. Chou, Structural supercapacitor composites: a review, Compos. Sci. Technol. 204 (2021) 108636.
[210] A. Borenstein, O. Hanna, R. Attias, S. Luski, T. Brousse, D. Aurbach, Carbon-based composite materials for supercapacitor electrodes: a review, J. Mater. Chem. A 5 (25) (2017) 12653–12672.

[211] Y. Guo, F. Qu, R. Tiwari, D.Y. Yoo, K. Wang, Y. Wang, Development of self-sensing asphalt cementitious composites using conductive carbon fibre and recycled copper tailing, Constr. Build. Mater. 474 (2025) 140965.

[212] Y. Guo, F. Qu, Advancing circular economy and construction sustainability: transforming mine tailings into high-value cementitious and alkali-activated concrete, npj Mater. Sustain. 3 (1) (2025) 8.

[213] Y. Song, L. Huang, Y. Wang, Y. Du, Z. Song, Q. Dong, X. Zhao, J. Qi, G. Zhang, W. Li, L. Shi. Energy performance and fire risk of solar PV panels under partial shading: An experimental study. Renew. Energy 246, 2025, 122910.

[214] Z. Luo, Y. Guo, C. Zhao, X. Wang, X. Zhang, V. Wu, W. Li. Nano/micro characterization on interfacial transition zones in fly ash–based geopolymer concrete, The Path to Green Concrete, Woodhead Publishing Series in Civil and Structural Engineering 2024, 445-475.

[215] C. Jin, J. Hu, J. Wu, H. Liang, J. Li, Innovative and economically beneficial use of corn and corn products in electrochemical energy storage applications, ACS Sustain. Chem. Eng. 9 (32) (2021) 10678–10703.

[216] K. Liang, Y. Chen, D. Wang, W. Wang, S. Jia, N. Mitsuzakic, Z. Chen, Post-modified biomass derived carbon materials for energy storage supercapacitors: a review, Sustainable Energy Fuels 7 (15) (2023) 3541–3559.

[217] L. Jiang, S.O. Han, M. Pirie, H.H. Kim, Y.-H. Seong, H. Kim, J.S. Foord, Seaweed biomass waste-derived carbon as an electrode material for supercapacitor, Energy Environ. 32 (6) (2021) 1117–1129.

[218] X. Li, J. Zhao, Z. Cai, F. Ge, A dyeing-induced heteroatom-co-doped route toward flexible carbon electrode derived from silk fabric, J. Mater. Sci. 53 (2018) 7735–7743.

[219] C. Liu, H. Wang, X. Zhao, H. Liu, Y. Sun, L. Tao, M. Huang, J. Shi, Z. Shi, Cellulose-derived carbon-based electrodes with high capacitance for advanced asymmetric supercapacitors, J. Power Sources 457 (2020) 228056.

[220] Y. Tong, J. Yang, J. Li, Z. Cong, L. Wei, M. Liu, S. Zhai, K. Wang, Q. An, Lignin-derived electrode materials for supercapacitor applications: progress and perspectives, J. Mater. Chem. A (2023).

[221] L. Wu, X. Shi, Z.S. Wu, Recent Advancements and Perspectives of Biodegradable Polymers for Supercapacitors, Adv. Funct. Mater. 2211454 (2023).

[222] V. García-Negrón, N.D. Phillip, J. Li, C. Daniel, D. Wood, D.J. Keffer, O. Rios, D. P. Harper, Processing–Structure–Property Relationships for Lignin-Based Carbonaceous Materials Used in Energy-Storage Applications, Energ. Technol. 5 (8) (2017) 1311–1321.

[223] Y. Xiao, Y. Wang, S.-H. Bo, J.C. Kim, L.J. Miara, G. Ceder, Understanding interface stability in solid-state batteries, Nat. Rev. Mater. 5 (2) (2020) 105–126.

[224] T. Watanabe, Y. Inafune, M. Tanaka, Y. Mochizuki, F. Matsumoto, H. Kawakami, Development of all-solid-state battery based on lithium ion conductive polymer nanofiber framework, J. Power Sources 423 (2019) 255–262.

[225] A. Bielefeld, D.A. Weber, J.R. Janek, Microstructural modeling of composite cathodes for all-solid-state batteries, J. Phys. Chem. C 123 (3) (2018) 1626–1634.

[226] B. Sun, X. Zhang, X. Fan, R. Wang, H. Bai, X. Wei, Interface modification based on MnO2@ N-doped activated carbon composites for flexible solid-state asymmetric supercapacitors, Energy 249 (2022) 123659.

[227] P. Braun, C. Uhlmann, M. Weiss, A. Weber, E. Ivers-Tiffée, Assessment of all-solid-state lithium-ion batteries, J. Power Sources 393 (2018) 119–127.

[228] L. Froboese, J.F. van der Sichel, T. Loellhoeffel, L. Helmers, A. Kwade, Effect of microstructure on the ionic conductivity of an all solid-state battery electrode, J. Electrochem. Soc. 166 (2) (2019) A318.

[229] J.A. Dawson, P. Canepa, T. Famprikis, C. Masquelier, M.S. Islam, Atomic-scale influence of grain boundaries on Li-ion conduction in solid electrolytes for all-solid-state batteries, J. Am. Chem. Soc. 140 (1) (2018) 362–368.

[230] E. Yi, H. Shen, S. Heywood, J. Alvarado, D.Y. Parkinson, G. Chen, S.W. Sofie, M. M. Doeff, All-solid-state batteries using rationally designed garnet electrolyte frameworks, ACS Appl. Energy Mater. 3 (1) (2020) 170–175.

[231] D.W. McOwen, S. Xu, Y. Gong, Y. Wen, G.L. Godbey, J.E. Gritton, T.R. Hamann, J. Dai, G.T. Hitz, L. Hu, 3D-printing electrolytes for solid-state batteries, Adv. Mater. 30 (18) (2018) 1707132.

[232] C. Yang, L. Zhang, B. Liu, S. Xu, T. Hamann, D. McOwen, J. Dai, W. Luo, Y. Gong, E.D. Wachsman, Continuous plating/stripping behavior of solid-state lithium metal anode in a 3D ion-conductive framework, Proc. Natl. Acad. Sci. 115 (15) (2018) 3770–3775.

[233] I. Dincer, M.A. Rosen, Exergy analysis of green energy systems, Green Energy: Basic Concepts and Fundamentals (2011) 17–65.